

The Gemini NICI Planet-Finding Campaign: Discovery of a Multiple System Orbiting the Young A Star HD 1160

Eric L. Nielsen,¹ Michael C. Liu,¹ Zahed Wahhaj,¹ Beth A. Biller,² Thomas L. Hayward,³ Alan Boss,⁴ Brendan Bowler,¹ Adam Kraus,^{1,5} Evgenya L. Shkolnik,⁶ Matthias Tecza,⁷ Mark Chun,¹ Fraser Clarke,⁷ Laird M. Close,⁸ Christ Ftaclas,¹ Markus Hartung,⁸ Jared R. Males,⁸ I. Neill Reid,⁹ Andrew J. Skemer,⁸ Silvia H. P. Alencar,¹⁰ Adam Burrows,¹¹ Elisabete de Gouveia Dal Pino,¹² Jane Gregorio-Hetem,¹² Marc Kuchner,¹³ Niranjana Thatte,⁶ Douglas W. Toomey¹⁴

ABSTRACT

We report the discovery by the Gemini NICI Planet-Finding Campaign of two low-mass companions to the young A0V star HD 1160 at projected separations of 81 ± 5 AU (HD 1160 B) and 533 ± 25 AU (HD 1160 C). VLT images of the system taken over a decade for the purpose of using HD 1160 A as a photometric calibrator confirm that both companions are physically associated. By comparing the system to members of young moving groups and open clusters with well-established ages, we estimate an

¹Institute for Astronomy, University of Hawaii, 2680 Woodlawn Drive, Honolulu HI 96822, USA

²Max-Planck-Institut für Astronomie, Königstuhl 17, 69117 Heidelberg, Germany

³Gemini Observatory, Southern Operations Center, c/o AURA, Casilla 603, La Serena, Chile

⁴Department of Terrestrial Magnetism, Carnegie Institution of Washington, 5241 Broad Branch Road, N.W., Washington, DC 20015, USA

⁵Hubble Fellow

⁶Lowell Observatory, 1400 West Mars Road, Flagstaff, AZ 86001, USA

⁷Department of Astronomy, University of Oxford, DWB, Keble Road, Oxford OX1 3RH, UK

⁸Steward Observatory, University of Arizona, 933 North Cherry Avenue, Tucson, AZ 85721, USA

⁹Space Telescope Science Institute, 3700 San Martin Drive, Baltimore, MD 21218, USA

¹⁰Departamento de Física - ICEx - Universidade Federal de Minas Gerais, Av. Antonio Carlos, 6627, 30270-901, Belo Horizonte, MG, Brazil

¹¹Department of Astrophysical Sciences, Peyton Hall, Princeton University, Princeton, NJ 08544

¹²Universidade de São Paulo, IAG/USP, Departamento de Astronomia, Rua do Matao, 1226, 05508-900, São Paulo, SP, Brazil

¹³NASA Goddard Space Flight Center, Exoplanets and Stellar Astrophysics Laboratory, Greenbelt, MD, 20771, USA

¹⁴Mauna Kea Infrared, LLC, 21 Pookela St., Hilo, HI 96720, USA

age of 50^{+50}_{-40} Myr for HD 1160 ABC. While the *UVW* motion of the system does not match any known moving group, the small magnitude of the space velocity is consistent with youth. Near-IR spectroscopy shows HD 1160 C to be an $M3.5 \pm 0.5$ star with an estimated mass of $0.22^{+0.03}_{-0.04} M_{\odot}$, while NIR photometry of HD 1160 B suggests a brown dwarf with a mass of $33^{+12}_{-9} M_{Jup}$. The very small mass ratio (0.014) between the A and B components of the system is rare for A star binaries, and would represent a planetary-mass companion were HD 1160 A to be slightly less massive than the Sun.

Subject headings: brown dwarfs — instrumentation: adaptive optics — planetary systems — planets and satellites: detection — stars: individual (HD 1160)

1. Introduction

There are almost 700 extrasolar planets discovered to date, most of them at small separations (< 5 AU) from their parent stars (e.g. Butler et al. 2006; Marcy et al. 2008; Mayor et al. 2009). In addition, 1235 transiting planet candidates have been discovered by NASA’s *Kepler* Mission (Borucki et al. 2011), effectively tripling the census of exoplanet candidates. Unlike radial velocity and transit surveys, which are responsible for the vast majority of these discoveries, direct imaging allows us to access planets at much larger separations ($\gtrsim 5$ AU). Direct imaging surveys for gas-giant planets around young stars initially returned null results (Lafrenière et al. 2007; Biller et al. 2007; Nielsen et al. 2008), and a detailed analysis of these null results shows that giant planets are rare at large ($\gtrsim 65$ AU) separations around solar-type stars (Nielsen & Close 2010). Despite the rarity of these objects, discoveries of directly imaged planets at large separations have now been announced (Marois et al. 2008, 2010; Kalas et al. 2008; Lafrenière et al. 2008; Lagrange et al. 2009; Kraus & Ireland 2012), allowing the study of the composition and formation of this new population of planets (e.g. Bowler et al. 2010; Currie et al. 2011; Barman et al. 2011).

High-mass stars have recently become exciting targets for direct imaging surveys. Both brown dwarfs (e.g. HR 7329 B [Lowrance et al. 2000] and HR 6037 B [Huélamo et al. 2010]) and planetary mass companions (HR 8799 bcde, Fomalhaut b, and Beta Pic b [Marois et al. 2010; Kalas et al. 2008; Lagrange et al. 2009]) have been detected around A-type stars. Analysis of radial-velocity results by Johnson et al. (2010) has shown that short-period ($a < 2.5$ AU) giant planets are more frequent around high-mass A stars than low-mass M stars, and the direct detection of planets around multiple A stars (where the higher contrast ratio should make planet detection by direct imaging more difficult) suggests this trend may continue to larger separations.

The Gemini NICI Planet-Finding Campaign is a 3-year survey begun in December 2008 targeting about 300 young, nearby stars to directly image extrasolar giant planets (Liu et al. 2010b). The goals of the Campaign are to detect new planets and to investigate the properties and formation mechanism of planets at $\gtrsim 10$ AU separations. Designed specifically to detect planets, the NICI instrument (Toomey & Ftacilas 2003; Chun et al. 2008) consists of an 85-element curvature adaptive

optics system, a Lyot coronagraph, and two cameras that can image simultaneously for spectral difference imaging (SDI; Racine et al. 1999), observing through two moderate-band filters around the H -band methane feature seen in cool substellar objects (Burrows et al. 1997; Baraffe et al. 2003). NICI also uses angular differential imaging (ADI), which holds the telescope rotator fixed, allowing speckle noise to be separated from real companions (Liu 2004; Marois et al. 2006).

We previously announced the Campaign discovery of two brown dwarfs orbiting young stars PZ Tel (Biller et al. 2010) and CD-35 2722 (Wahhaj et al. 2011). We present here the discovery of two low-mass companions to the young A star HD 1160, at ~ 80 AU (B) and ~ 530 AU (C) separations. HD 1160 (see Table 1) is a well known photometric standard star from Elias et al. (1982) and was selected for the Campaign due to its underluminous position on the HR diagram, a sign of youth for field A stars (e.g. Jura et al. 1998). HD 1160 was observed by Su et al. (2006) with *Spitzer* at $24\ \mu\text{m}$, and no excess was detected. We derive an age range for the system of 50^{+50}_{-40} Myr and estimate masses for the two companions of $33^{+12}_{-9}\ M_{\text{Jup}}$ (HD 1160 B) and $0.22^{+0.03}_{-0.04}\ M_{\odot}$ (HD 1160 C).

2. Observations

2.1. Gemini-South NICI: Near-Infrared Imaging

NICI, the Near Infrared Coronagraphic Imager, is a dual-channel high contrast imager at Gemini South, designed specifically to directly image giant planets. The detectors in the two channels are 1024×1024 Aladdin II InSb, with a square $18.43''$ field of view and 17.94 and 17.96 mas pixels in the two cameras.

HD 1160 was first observed on 2010 October 30 UT in the standard NICI Campaign observing modes (previously described in Biller et al. 2010 and Wahhaj et al. 2011). In the combined angular and spectral difference imaging (ASDI) mode, where we are more sensitive to methane-bearing planets, images are taken simultaneously in the 4% bandpass methane on ($1.652\ \mu\text{m}$) and off ($1.578\ \mu\text{m}$) filters using NICI’s two cameras. In the ADI mode, where all of the light is sent to one camera, we are more sensitive to faint companions at separations $\gtrsim 2''$. We obtained 45 1-minute exposure images in the ASDI mode and 20 1-minute exposure images in the ADI mode. In the ASDI mode, the primary is not saturated as it is observed through a partially transmissive coronagraphic mask at NICI’s first focal plane.

We easily detected two companions at separations of $0.78 \pm 0.03''$ and $5.15 \pm 0.03''$. After using archival VLT data to confirm that both companions are common proper motion (Sections 2.3 and 3.1), we observed HD 1160 again on UT November 22, 2010 in the J , H and K_S bands (filters are in the MKO system) in order to measure colors for the companions. Ten images were taken simultaneously in the H and K_S bands with exposure times of 12.16 seconds and 5 coadds per image. In the J -band, we obtained twenty images in single channel mode with the same exposure

times and coadds per image. Both companions were well detected even in individual images, but we chose only the best 7–10 images where the primary was centered most accurately on the mask. We obtained an additional NICI dataset on UT October 21, 2011 (in the narrowband methane filters), which provided further astrometric confirmation.

2.2. Keck-II NIRC2: L' and M_S band imaging

We observed HD 1160 in the L' (3.426–4.126 μm) and M_S (4.549–4.790 μm) bands with the Keck II Telescope adaptive optics system and facility near-IR camera NIRC2 on UT November 27, 2010 without any coronagraphic mask. We used the narrow camera which has 9.961 mas pixels (Ghez et al. 2008). In the direct imaging mode (non-ADI), we obtained 37 images at L' band, each with an exposure time of 0.15 seconds and 200 coadds. In the M_S band, we obtained 29 images with an exposure times of 0.2 seconds and 50 coadds. For each band, we used 5 dither positions with separations of 1". The median combination of the unshifted images was used to make sky images for subtraction. Both companions were clearly detected and the primary was unsaturated in both bands. In addition to the plate scale, we also use the Keck NIRC2 field rotation derived by Ghez et al. (2008) to determine the astrometry of the two companions.

2.3. VLT NACO and ISAAC: K_S , L , and L' imaging

We examined archival data of HD 1160 taken at the VLT between 2002 and 2012 in order to assess whether HD 1160 B and C are common proper motion companions to HD 1160 A. These datasets include K_S and L' (3.49–4.11 μm) adaptive optics images taken with the NACO system, and ISAAC K_S and L (3.49–4.07 μm) images, originally obtained for photometric calibration of observations of other science targets. NACO images taken in the K_S -band have 27.06 mas pixels, while L' images have 27.12 mas pixels. ISAAC has a K_S pixel size of 148 mas and L -band images have a pixel size of 71 mas. Despite their relatively short integration times (of order one minute per epoch), HD 1160 C ($\sim 5''$ separation) is cleanly detected in all the data. HD 1160 B ($\sim 0.8''$ separation) is only detected in the adaptive optics datasets and is not resolved in the seeing-limited ISAAC data. Position angles measured with the NACO instrument are corrected to account for a -0.6 degree field rotation measured by Bergfors et al. (2011).

Figure 1 shows the detection of both companions at each VLT NACO, Gemini NICI, and Keck NIRC2 epoch. Figure 2 shows the detections of only HD 1160 C at each of the seven ISAAC epochs. Astrometry for all epochs is presented in Table 2.

2.4. Magellan MIKE: Optical Spectroscopy

We acquired a spectrum of HD 1160 A and C on UT 30 December 2010 with the Magellan Inamori Kyocera Echelle (MIKE) spectrograph at the Magellan Clay telescope at Las Campanas Observatory in Chile. We used the $0.5''$ slit which produces a spectral resolution of $\approx 35,000$. These data were reduced using the facility pipeline (Kelson 2003). We do not attempt to recover the spectrum of the much closer companion, HD 1160 B, with these observations.

Each stellar exposure is bias-subtracted and flat-fielded for pixel-to-pixel sensitivity variations. After optimal extraction, the 1-D spectra are wavelength calibrated with a thorium-argon arc. To correct for instrumental drifts, we used the telluric molecular oxygen A band (from 7620–7660 Å) which aligns the MIKE spectra to 40 m s^{-1} , after which we corrected for the heliocentric velocity. The final spectra are of moderate S/N reaching ≈ 50 per pixel at 8700 Å. We also observed GJ 908 (Spectral Type M1) as a radial velocity (RV) standard.

To measure the RV of HD 1160 C, we cross-correlated each of 9 orders between 7000 and 9000 Å (excluding those with strong telluric absorption) with the spectrum of GJ 908 using IRAF’s¹ *fxcor* routine (Fitzpatrick 1993). We use GJ 908’s $-71.147 \text{ km s}^{-1}$ RV published by the California and Carnegie Planet Search (Nidever et al. 2002). The zero-point of the absolute RV is uncertain at the 0.4 km s^{-1} level. We measured the RV of HD 1160 C from the gaussian peak fitted to the cross-correlation function (CCF) of each order and adopt the average RV of all orders with the standard deviation of the individual measurements. We measure the radial velocity of HD 1160 C to be $12.6 \pm 0.3 \text{ km/s}$. We also observed HD 1160 A itself with the MIKE spectrograph. Given the few spectral lines available we were unable to get as precise an RV measurement as we did for the M dwarf HD 1160 C. However, measuring the RV of several lines in HD 1160 A and taking the average, we found that the RV of HD 1160 A is $14 \pm 2 \text{ km/s}$, consistent with that of HD 1160 C.

2.5. IRTF SpeX: Near-IR Spectroscopy

We obtained moderate-resolution ($R \approx 2000$) near-IR spectra of HD 1160 A and C on 29 June 2011 UT from NASA’s Infrared Telescope Facility (IRTF), located on Mauna Kea, Hawaii. Conditions were photometric with good seeing conditions ($\approx 0.5\text{--}0.6''$), and the C companion was well-resolved from the primary star. We did not attempt to recover the spectrum of the much closer companion, HD 1160 B, with these observations.

We used the facility near-IR spectrograph SpeX (Rayner et al. 1998) with the $0.3''$ wide slit in cross-dispersed mode, obtaining spectra from $0.8\text{--}2.5 \mu\text{m}$. The slit was oriented at a position

¹IRAF (Image Reduction and Analysis Facility) is distributed by the National Optical Astronomy Observatories, which is operated by the Association of Universities for Research in Astronomy, Inc. (AURA) under cooperative agreement with the National Science Foundation.

angle of 50° on the sky, compared to the parallactic angle of $\approx 80^\circ$ at the time, in order to minimize the light from the primary that entered the slit. In the pairwise-subtracted images, in the H and K bands, no evidence was seen of contaminating light from the primary compared to the very well-detected companion. Some contamination was seen in the J band. Since the target was nearly overhead at the time of the observation (airmass ranging from 1.07 to 1.10), the effect of atmospheric dispersion on the broadband spectrum is minimal. The slit was not oriented perpendicular to the primary-companion axes, since this would cause the companion’s spatial position in the slit to coincide with a local maximum in the light from the primary’s halo.

HD 1160 C was nodded along the slit in an ABBA pattern for a total on-source integration of 16 min, with individual exposure times of 120 sec. We observed the primary star HD 1160 itself for telluric calibration, since it has a spectral type of A0V and was well-resolved from the companion. All spectra were reduced using version 3.4 of the SpeXtool software package (Vacca et al. 2003; Cushing et al. 2004). The median S/N per pixel in the final reduced spectrum is 25.

3. Results

3.1. Astrometric Confirmation of HD 1160 B and C

Our full set of astrometry from VLT, Gemini-South, and Keck is reported in Table 2. Figures 3 and 4 show the relative positions of HD 1160 B and C with respect to A over nearly a decade (2002–2011), along with the expected relative motion of a distant background object, given the known proper motion and parallax of HD 1160 A. Errors on this astrometric track are computed through a Monte Carlo approach, using errors from the reference (NICI, epoch 2010.8301) position, and errors in the proper motion and parallax of HD 1160 A from Hipparcos (van Leeuwen 2007).

Figures 5 and 6 show the astrometry of the companions on the sky. The astrometric measurements cluster on top of each other, as expected for common proper motion companions (CPM), and do not follow the background track.

To robustly determine whether each companion is more consistent with background or common proper motion, we compute the χ^2 statistic using the equations

$$\chi_{bg}^2 = \sum_i \left(\frac{(\rho_{obs,i} - \rho_{bg,i})^2}{\sigma_{\rho,i}^2} + \frac{(PA_{obs,i} - PA_{bg,i})^2}{\sigma_{PA,i}^2} \right) \quad (1)$$

and

$$\chi_{CPM}^2 = \sum_i \left(\frac{(\rho_{obs,i} - \rho_0)^2}{\sigma_{\rho,i}^2} + \frac{(PA_{obs,i} - PA_0)^2}{\sigma_{PA,i}^2} \right) \quad (2)$$

where $\rho_{obs,i}$ and $PA_{obs,i}$ are the observed separation and position angle at each epoch (i), $\rho_{bg,i}$ and $PA_{bg,i}$ are the expected separation and position angle at each epoch from the background (bg) track, ρ_0 and PA_0 are constant separations and position angles (corresponding to common proper motion), and $\sigma_{\rho,i}$ and $\sigma_{PA,i}$ are the measurement uncertainties in the observed separation and position angle.

HD 1160 B is easily confirmed as a co-moving companion, differing from the expected motion of a background object by 15 degrees in position angle. The fit to the background track across all epochs has reduced chi square $\chi^2_\nu=26.2$ (with 22 degrees of freedom). These data are not consistent with the background hypothesis, which is ruled out at the $P \approx 0\%$ level. Meanwhile, the fit to constant separation and position angle (i.e. common proper motion) produces $\chi^2_\nu=0.38$ (dof=22, $P=99.6\%$). The deviation of HD 1160 C’s motion from the background track is less than that for B. Nevertheless the offsets are significantly more consistent with common proper motion ($\chi^2_\nu=0.62$, dof=36, $P=96.5\%$) than background ($\chi^2_\nu=4.95$, dof=36, $P \approx 0\%$). Though examining Figure 6 shows that while there is a spread to the 19 astrometric epochs and they do not clearly overlap within error bars, the direction of the spread is orthogonal to the expected motion of a background object (and probably due to orbital motion, as we discuss below. In addition, we note that the radial velocity measurements of HD 1160 A and HD 1160 C are consistent within measurement uncertainties (see Section 2.4), as we would expect from physically associated companions.

Figure 4 suggests a small change in position angle over time for HD 1160 C, raising the possibility that we are observing orbital motion. Fitting a straight line with non-zero slope to the astrometry for HD 1160 C produces $\chi^2_\nu=0.42$ (dof=34, $P=99.8\%$), similar to the common proper motion fit, indicating that with our astrometric errors, we are unable to detect a deviation from non-zero relative motion. Assuming a mass for an A0 star of $2.2 M_\odot$ (Siess et al. 2000), a mass for HD 1160 C of $0.2 M_\odot$ (see Section 3.6), and a face-on circular orbit with semi-major axis of the projected separation of 531 AU, we would expect orbital motion of $\sim 0.05^\circ/\text{year}$, while the best-fit line to the PA motion gives $-0.04 \pm 0.03^\circ/\text{year}$. So while we do not significantly detect orbital motion, the magnitude of such motion would be consistent with that expected for HD 1160 C.

3.2. Spectral Typing of HD 1160 C

Figure 7 shows the $H-K$ and $K-L'$ colors for HD 1160 B and C compared to field objects of M and L spectral types. The locations of the HD 1160 companions in this color-color diagram suggest spectral types of mid-M for HD 1160 C, and late M/early L for HD 1160 B.

Figure 8 shows HD 1160 B and C on an MKO NIR color-color diagram that includes field stars, field L dwarfs, selected individual low-mass objects, and members of the Taurus star-forming region. We include in this plot photometry of field stars (Rayner et al. 2009) and field L-dwarfs (Leggett et al. 2010), as well as the low mass objects AB Pic b (Chauvin et al. 2005), G 196-3 B (Rebolo et al. 1998), PZ Tel B (Biller et al. 2010), 2M 1207 A (Mohanty et al. 2007), and TWA 5B

(Lowrance et al. 1999). In addition, we plot JHK photometry for a list of spectroscopically confirmed Taurus members that do not possess circumstellar disks (Luhman et al. 2010) or known binary companions (Kraus et al. 2011, 2012). The JHK photometry (taken from 2MASS) has been dereddened using the extinction values from the compilation of Kraus & Hillenbrand (2009) or the discovery survey, using the relative extinctions from Schlegel et al. (1998), and converted to MKO using the conversion of Leggett et al. (2006).

Rayner et al. (2009) note that this figure bifurcates for field dwarfs and giants with M spectral types; and indeed, while some giants are on the lower sequence, no field M dwarfs are found on the upper sequence. HD 1160 B and C fall clearly on the upper branch with the M giants, and not the lower branch with the M dwarfs. HD 1160 B and C cannot be giant stars themselves, as this would be inconsistent with their absolute magnitudes. A small fraction of the Taurus objects lie on the upper sequence, but most lie on the lower branch. That so few of these young ($\sim 2\text{--}5$ Myr) objects fall on the upper branch appears to rule out the possibility that young objects (with intermediate surface gravity between giants and dwarfs) populate the upper branch and older objects the lower one. Other plausible explanations for the five Taurus objects with giant-like colors include the presence of an undetected binary or disk, or an incorrect reddening determination. Or, perhaps some small fraction of young stars lie on the upper branch, while most lie on the lower branch. Alternatively, the discrepancy could also be accounted for by an error in our photometric reduction: shifting our NICI photometry of HD 1160 B and C by $\sim 2\sigma$ would also place both objects on the lower track. In any case, with our current data we are unable to explain why the JHK photometry of HD 1160 B and C diverges from the photometry of dwarfs and the bulk of the single-star diskless Taurus objects.

To assign a spectral type for HD 1160 C, we plot our IRTF/SpeX spectrum against M-dwarf standards from Cushing et al. (2005) in Figure 9. We match flux levels for the entire JHK spectrum using only the H and K portions of the spectra, since our J -band data is particularly noisy and likely contaminated by HD 1160 A. The best match to the shape of the continuum and spectral features comes from the M3 and M4 templates. As a result, we assign a spectral type of $M3.5 \pm 0.5$ to HD 1160 C.

We have also compared the spectrum of HD 1160 C to an M3.5 III spectrum from Cushing et al. (2005), but find a poor fit to the IRTF/SpeX spectrum, for both the shape of the continuum and strength of the absorption features. This is as we would expect: HD 1160 C, while having NIR colors similar to a giant, is not a giant itself.

Figure 10 compares the equivalent widths of atomic features for HD 1160 C with those for stars from Rayner et al. (2009) and members of the ~ 10 Myr TW Hydra Association (Covey et al. 2010). As in Rayner et al. (2009), we follow the method of Cushing et al. (2005) to compute equivalent widths and associated errors (see their Section 3.4), by defining continuum regions, fitting a polynomial, and directly computing the flux difference between measured spectrum and estimated continuum in the line regions. A spectral type of M3.5V is consistent with HD 1160 C.

We cannot use these data to constrain the age, since at a spectral type of M3.5, there is not a significant offset between the field M dwarfs and young M stars in TWA in the strength of the absorption lines.

3.3. Age of the HD 1160 System

Determining the age of the HD 1160 system is challenging, since the most widely used age diagnostics (such as lithium absorption, calcium emission, $H\alpha$ emission, and rotation rate) are suitable only for stars with spectral types of F, G, and K (e.g. Soderblom 2010). In the case of HD 1160 ABC, with spectral types A, L, and M, none of the components are amenable to these techniques for determining ages, and so we turn to an analysis of the system’s position on the HR diagram to estimate its age. In fact, this is a more fundamental method of determining ages, since lithium and other indirect age indicators are calibrated by measurements from open clusters, whose ages are determined by comparison to isochrones on the HR diagram.

HD 1160 A was originally selected as a target for the Gemini NICI Planet-Finding Campaign due to its faint absolute magnitude for its spectral type. Jura et al. (1998) and Lowrance et al. (2000) note that on the HR diagram early-type stars in young clusters tend to be lower (i.e. have smaller luminosities) than stars in older clusters. In fact, Su et al. (2006) flag HD 1160 A as lying below the zero-age main sequence, implying an age of <5 Myr. (HR 8799, the host of 4 directly imaged planets, was determined to be young by the same method [Marois et al. 2008].) With our discovery of two co-moving companions to HD 1160 A, we can expand this HR diagram analysis to include all three components, with spectral types ranging from A0 to early L.

Figure 11 shows HD 1160 A and C compared to stars at six sets of ages: Upper Sco (Kraus & Hillenbrand 2008) at 5 Myr; members of ~ 10 Myr (β Pic and TW Hya) and ~ 30 Myr (Tuc/Hor, Carina, and Columba) moving groups (Torres et al. 2008); the 120 Myr Pleiades open cluster (Stauffer et al. 2007); the Hyades open cluster (Röser et al. 2011) at 600 Myr; and low-mass field objects from the Palomar/MSU Nearby-Star Spectroscopic Survey (Hawley et al. 1996). All NIR photometry of reference objects were obtained with 2MASS filters, and so we use the conversion factors of Leggett et al. (2006) to convert the HD 1160 ABC MKO magnitudes into 2MASS magnitudes for Figure 11 (we do the same for Figure 12). As we currently lack spectra for HD 1160 B and cannot determine its spectral type, we do not plot it in Figure 11. From these plots, the HD 1160 system appears younger than the Hyades (given the low luminosity of HD 1160 A with respect to the Hyades A star sequence), but consistent with the younger associations.

In Figure 12, we show a NIR color-magnitude diagram for the same associations, along with all three members of the HD 1160 system. Here, HD 1160 again appears younger than the Hyades and the field objects, and inconsistent with the Pleiades as well, with HD 1160 A below the A-star sequence, and HD 1160 B and C redder than M stars of similar absolute J magnitudes. All three components are consistent with similar objects in Upper Sco or the 10 and 30 Myr moving groups

(though the paucity of known low-mass members to the two sets of moving groups makes a detailed comparison at these ages difficult). As a result, we set an upper limit for the age of the HD 1160 system of 100 Myr, and adopt an age range of 50_{-40}^{+50} Myr.

3.4. Metallicity

An alternate explanation for the underluminosity of HD 1160 A is that the system has a sub-solar metallicity, as we illustrate in Figure 13. While HD 1160 A lies below the Siess et al. (2000) tracks at $[\text{Fe}/\text{H}] = 0.0$, its position on the color-magnitude diagram is consistent for ages up to 300 Myr at $[\text{Fe}/\text{H}] = -0.3$, half the metal abundance of the Sun. Similarly, Merín et al. (2004) found that the low position of HD 141569 (a pre-main sequence B9.5V with a circumstellar disk) on the HR diagram as well as its medium-resolution optical spectrum could be explained by a metallicity of $[\text{Fe}/\text{H}] = -0.5$.

We note, however, that Figure 12 provides two indications of youth for HD 1160: the underluminosity of A and the redness of B and C in $J - K_S$ color. In Figure 14 we show a NIR color-magnitude diagram with HD 1160 B and C and field M dwarfs of known metallicity (Leggett et al. 2000; Rojas-Ayala et al. 2010). M dwarfs with subsolar metallicity have bluer $J - K_S$ colors than more metal-rich M dwarfs. So if the HD 1160 system were to be old (>100 Myr) but metal-poor, we would expect bluer $J - K_S$ colors for HD 1160 B and C than we observe. The underluminosity of A stars on color-magnitude diagrams may indicate either young age or low metallicity, but the only available explanation for red $J - K_S$ colors in late-type stars is youth. Indeed, Johnson et al. (2011) derive a relationship between $J - K_S$ color and metallicity of M dwarfs, with redder $J - K_S$ color indicating more metal-rich atmospheres.

We also note that regardless of whether HD 1160 A has $[\text{Fe}/\text{H}] = 0.0$ or -0.3 , the expected main sequence lifetime of an A0 star is ~ 300 Myr (Siess et al. 2000), which provides an upper limit on the age of the system independent of the measured photometry of HD 1160 B and C. Additionally, since stars recently formed in the solar neighborhood tend to be of solar metallicity (Pedicelli et al. 2009), for an age less than ~ 300 Myr, the HD 1160 system would have had to have formed further out in the galactic disk (i.e. in a lower metallicity environment) and migrated inward, which is inconsistent with its main sequence lifetime of ~ 300 Myr and its low space motion (see Section 3.5). Though a metallicity of $[\text{Fe}/\text{H}] = -0.3$ is at the lower limit of Cepheids at the solar radius, as measured by Pedicelli et al. (2009), the more likely explanation is that HD 1160 A is solar metallicity, and its low position in the HR diagram is due to youth.

3.5. Space Motion

By combining our measured RV of the HD 1160 system with the position and revised Hipparcos parallax and proper motion of HD 1160 A (van Leeuwen 2007), we have computed the space motion

of HD 1160. We find the space motion to be $U = 7.6 \pm 0.4$, $V = -3.4 \pm 0.5$, $W = -15.7 \pm 0.4$ km/s. In Figure 15, we compare this space motion to those of young, nearby moving groups, as given by Torres et al. (2008). HD 1160 is not co-moving with any known moving group, though its space motion is relatively low, with a total motion of 17.7 ± 0.5 km/s. Such a low velocity is consistent with a young age for HD 1160. We also note that this UVW motion of HD 1160 places the system slightly outside (though near the edge) of the 1σ UVW ellipse of the “young disk” computed by Eggen (1989) of $U = 15 \pm 14$, $V = -14 \pm 9$, $W = -6 \pm 13$ km/s.

3.6. Mass of HD 1160 B and C

Using the age and available photometry and spectroscopy of HD 1160 B and C, we proceed to assign masses to these companions using theoretical evolutionary models for stellar and sub-stellar objects. Table 4 shows mass estimates from the Lyon evolutionary models using the DUSTY atmospheric models (Chabrier et al. 2000; Allard et al. 2001) for HD 1160 B for the absolute magnitudes in each infrared band. Errors are calculated by interpolation across gridpoints of the DUSTY models, and using a Monte Carlo analysis assuming gaussian distributions for the magnitude uncertainties and a uniform distribution of ages from 10–100 Myr. Given the large age range, the implied mass range is quite large (24–90 M_{Jup}), spanning much of the range of brown dwarf masses. We note that these ranges only account for uncertainties in fluxes and the age, and do not account for any systematic uncertainty in the models themselves. From the J -band (the peak of the NIR SED for late M and early L spectral types) flux alone, we derive a mass for HD 1160 B of $33^{+12}_{-9} M_{Jup}$. Using the $BC(J)$ bolometric correction of Liu et al. (2010a) ($BC(J)$ chosen since it is flat over the plausible range of spectral type for HD 1160 B, $L0 \pm 2$), we find a similar mass by computing the bolometric luminosity ($L = 5.9 \times 10^{-4} \pm 5 \times 10^{-5} L_{\odot}$), and comparing to the DUSTY models: $M = 37^{+12}_{-10} M_{Jup}$.

For HD 1160 C, we incorporate our measured spectral type of $M3.5 \pm 0.5$ when estimating the mass. Using the dwarf sequence of Luhman (1999), we convert this spectral type to an effective temperature of 3270 ± 90 K, (or 3340 ± 70 K using the intermediate scale) and using a K-band bolometric correction from Golimowski et al. (2004), we compute a luminosity of HD 1160 C of $9.4 \times 10^{-3} \pm 8 \times 10^{-4} L_{\odot}$. Coupled with the NextGen models of Baraffe et al. (1998), these values allow us to estimate a mass for HD 1160 C of $190^{+65}_{-40} M_{Jup}$. Using the Luhman (1999) intermediate sequence (more appropriate for younger stars), we find the mass of HD 1160 C to be $230^{+30}_{-45} M_{Jup}$ ($0.22^{+0.03}_{-0.04} M_{\odot}$).

3.7. Orbital Stability

We estimate the likely semimajor axes of the two companions from their projected separations using the conversion factor of Dupuy & Liu (2011): assuming a uniform eccentricity distribution

between 0 and unity and no discovery bias, their estimated ratio of semi-major axis (a) to projected separation (ρ) is $a/\rho = 1.10$ with 68.3% confidence limits between 0.75 and 2.02. Given projected separations of 81 ± 5 AU and 533 ± 25 AU for HD 1160 B and C, and using a Monte Carlo method to propagate errors (using a gaussian distribution for separation and two gaussians to account for the assymetric error bars on a/ρ), we estimate semi-major axes of 74 ± 35 AU for HD 1160 B and 500 ± 200 for HD 1160 C.

The HD 1160 ABC system appears to be orbitally stable, assuming that the eccentricity of the A and C components is not larger than about 0.3. Given the mass ratio between HD 1160 A and C of 0.1, and using the detailed orbital stability calculations of Holman & Wiegert (1999), and assuming an orbital eccentricity of these two major components of 0.3, we estimate that for the HD 1160 system the critical semimajor axis for stability of component B is about 0.2 times the semimajor axis of components A and C. That is, component B can orbit no farther from A than about 100 AU. With an estimated semi-major axis of about 74 AU, component B therefore appears to be part of a stable hierarchical system. Smaller orbital semimajor axes for HD 1160 B would also be stable, and so additional companions could plausibly exist interior to B.

Since we have not fit an orbital solution to our astrometry, the semi-major axes of both components may differ from our estimates. Indeed, if the semi-major axis is 109 AU for HD 1160 B and 300 AU for HD 1160 C (the 1σ upper and lower limits of their respective semi-major axis estimates), then the system would not be orbitally stable. Additionally, a high eccentricity for one or both of HD 1160 B and C would suggest instability. Nevertheless, given our measurements, and the small probability of catching this system in an unstable state, the most likely explanation is that the system is stable.

4. Conclusions

We have described here the discovery and analysis of two low-mass companions to the young A star HD 1160 A, found during the Gemini NICI Planet-Finding Campaign. With estimated companion masses of 33^{+12}_{-9} and $230^{+30}_{-45} M_{Jup}$ and a primary mass of $\sim 2.2 M_{\odot}$, this system has very small mass ratios between components, 0.10 between A and C, and 0.014 between A and B. Around a star slightly less massive than the Sun, this A-to-B mass ratio would represent a planetary-mass companion.

Hierarchical triple systems like HD 1160 occur with a frequency of about 8% around solar-type stars (Raghavan et al. 2010), though seldom with such extreme mass ratios as the A to B components of HD 1160. Mass ratios less than about 0.1 are rare (see Figure 16 of Raghavan et al. 2010) though not unprecedented, e.g., ζ Vir B, an M-dwarf companion to an A star, with mass ratio 0.08 (Hinkley et al. 2010) resembles HD 1160 C, while the brown dwarf HR 7329 B, with mass ratio of ~ 0.01 relative to its A-star primary (Lowrance et al. 2000), is more akin to HD 1160 B. Along with binary star systems, multiple star systems like HD 1160 are thought to form by the

collapse and fragmentation of dense molecular cloud cores (e.g., Boss 2009 and references therein). The cloud core that collapsed to form HD 1160 presumably was relatively rapidly rotating, in order to result in the wide orbits of all three components. Typical separations for binary stars with mass ratios of about 0.1 (as for A and C) are in the range of about 10 to 10^4 AU (see Figure 17 of Raghavan et al. 2010), so a separation of A and C of about 531 AU is consistent with this range.

Near-IR spectra of HD 1160 B will likely set much stronger constraints on the age of the system, as an \sim L0 brown dwarf (as suggested by the photometry shown in Figure 7) will show significant spectral evolution up to the main sequence lifetime of HD 1160 A (\sim 300 Myr). If the spectrum shows signs of low surface gravity compared to field L dwarfs (e.g. McGovern et al. 2004; Allers et al. 2007, 2009), this will help refine our age determination of the system.

In the longer term, high-precision orbital monitoring of both components may be able to constrain the orbital parameters of HD 1160 B and C. Given the expected orbital periods of \sim 400 and \sim 7000 years, such orbital motion will be quite small and so will require high precision and long time baselines. In fact, the orbital period of HD 1160 B may be significantly longer than 400 years, since a circular face-on orbit would predict \sim 120 mas of motion over the 10 years for which we have archival data, and a linear fit to the relative motion of HD 1160 B gives only 23 ± 29 mas over 10 years ($< 1\sigma$, so not a significant detection of orbital motion). The fact that we observe a larger degree of orbital motion from the further-out C (60 ± 30 mas over 10 years) than from the close-in B suggests that there may be significant misalignment of the orbital planes of these two companions. Additional follow-up and analysis of this system will set interesting constraints for modeling the formation of HD 1160 ABC.

B.A.B was supported by Hubble Fellowship grant HST-HF-01204.01-A awarded by the Space Telescope Science Institute, which is operated by AURA for NASA, under contract NAS 5-26555. This work was supported in part by NSF grants AST-0713881 and AST-0709484. The Gemini Observatory is operated by the Association of Universities for Research in Astronomy, Inc., under a cooperative agreement with the NSF on behalf of the Gemini partnership: the National Science Foundation (United States), the Science and Technology Facilities Council (United Kingdom), the National Research Council (Canada), CONICYT (Chile), the Australian Research Council (Australia), CNPq (Brazil), and CONICET (Argentina). Based on observations made with the European Southern Observatory telescopes obtained from the ESO/ST-ECF Science Archive Facility. This publication makes use of data products from the Two Micron All Sky Survey, which is a joint project of the University of Massachusetts and the Infrared Processing and Analysis Center/California Institute of Technology, funded by the National Aeronautics and Space Administration and the National Science Foundation. This research has made use of the SIMBAD database, operated at CDS, Strasbourg, France. This research has made use of the VizieR catalogue access tool, CDS, Strasbourg, France. Some of the data presented herein were obtained at the W.M. Keck Observatory, which is operated as a scientific partnership among the California Institute of Technology, the University of California and the National Aeronautics and Space Administration.

The Observatory was made possible by the generous financial support of the W.M. Keck Foundation. This paper uses data from the Infrared Telescope Facility, which is operated by the University of Hawaii under Cooperative Agreement no. NNX-08AE38A with the National Aeronautics and Space Administration, Science Mission Directorate, Planetary Astronomy Program.

Facilities: Gemini:South (NICI), Keck II (NIRC2), VLT:Yepun (NACO), VLT:Melipal (ISAAC), IRTF (SpeX), Magellan II (MIKE).

REFERENCES

- Allard, F., Hauschildt, P. H., Alexander, D. R., Tamanai, A., & Schweitzer, A. 2001, *ApJ*, 556, 357
- Allers, K. N., Jaffe, D. T., Luhman, K. L., Liu, M. C., Wilson, J. C., Skrutskie, M. F., Nelson, M., Peterson, D. E., Smith, J. D., & Cushing, M. C. 2007, *ApJ*, 657, 511
- Allers, K. N., Liu, M. C., Shkolnik, E., Cushing, M. C., Dupuy, T. J., Mathews, G. S., Reid, I. N., Cruz, K. L., & Vacca, W. D. 2009, *ApJ*, 697, 824
- Baraffe, I., Chabrier, G., Allard, F., & Hauschildt, P. 2003, in *IAU Symposium*, Vol. 211, *Brown Dwarfs*, ed. E. Martín, 41–+
- Baraffe, I., Chabrier, G., Allard, F., & Hauschildt, P. H. 1998, *A&A*, 337, 403
- Barman, T. S., Macintosh, B., Konopacky, Q. M., & Marois, C. 2011, *ApJ*, 733, 65
- Bergfors, C., Brandner, W., Janson, M., Köhler, R., & Henning, T. 2011, *A&A*, 528, A134
- Biller, B. A., Close, L. M., Masciadri, E., Nielsen, E., Lenzen, R., Brandner, W., McCarthy, D., Hartung, M., Kellner, S., Mamajek, E., Henning, T., Miller, D., Kenworthy, M., & Kulesa, C. 2007, *ApJS*, 173, 143
- Biller, B. A., Liu, M. C., Wahhaj, Z., Nielsen, E. L., Close, L. M., Dupuy, T. J., Hayward, T. L., Burrows, A., Chun, M., Ftaclas, C., Clarke, F., Hartung, M., Males, J., Reid, I. N., Shkolnik, E. L., Skemer, A., Tecza, M., Thatte, N., Alencar, S. H. P., Artymowicz, P., Boss, A., de Gouveia Dal Pino, E., Gregorio-Hetem, J., Ida, S., Kuchner, M. J., Lin, D., & Toomey, D. 2010, *ApJ*, 720, L82
- Borucki, W. J., Koch, D. G., Basri, G., Batalha, N., Brown, T. M., Bryson, S. T., Caldwell, D., Christensen-Dalsgaard, J., Cochran, W. D., DeVore, E., Dunham, E. W., Gautier, III, T. N., Geary, J. C., Gilliland, R., Gould, A., Howell, S. B., Jenkins, J. M., Latham, D. W., Lissauer, J. J., Marcy, G. W., Rowe, J., Sasselov, D., Boss, A., Charbonneau, D., Ciardi, D., Doyle, L., Dupree, A. K., Ford, E. B., Fortney, J., Holman, M. J., Seager, S., Steffen, J. H., Tarter, J., Welsh, W. F., Allen, C., Buchhave, L. A., Christiansen, J. L., Clarke, B. D., Das, S., Désert, J.-M., Endl, M., Fabrycky, D., Fressin, F., Haas, M., Horch, E., Howard, A.,

- Isaacson, H., Kjeldsen, H., Kolodziejczak, J., Kulesa, C., Li, J., Lucas, P. W., Machalek, P., McCarthy, D., MacQueen, P., Meibom, S., Miquel, T., Prsa, A., Quinn, S. N., Quintana, E. V., Ragozzine, D., Sherry, W., Shporer, A., Tenenbaum, P., Torres, G., Twicken, J. D., Van Cleve, J., Walkowicz, L., Witteborn, F. C., & Still, M. 2011, *ApJ*, 736, 19
- Boss, A. P. 2009, *ApJ*, 697, 1940
- Bowler, B. P., Liu, M. C., Dupuy, T. J., & Cushing, M. C. 2010, *ApJ*, 723, 850
- Burrows, A., Marley, M., Hubbard, W. B., Lunine, J. I., Guillot, T., Saumon, D., Freedman, R., Sudarsky, D., & Sharp, C. 1997, *ApJ*, 491, 856
- Butler, R. P., Wright, J. T., Marcy, G. W., Fischer, D. A., Vogt, S. S., Tinney, C. G., Jones, H. R. A., Carter, B. D., Johnson, J. A., McCarthy, C., & Penny, A. J. 2006, *ApJ*, 646, 505
- Chabrier, G., Baraffe, I., Allard, F., & Hauschildt, P. 2000, *ApJ*, 542, 464
- Chauvin, G., Lagrange, A.-M., Zuckerman, B., Dumas, C., Mouillet, D., Song, I., Beuzit, J.-L., Lowrance, P., & Bessell, M. S. 2005, *A&A*, 438, L29
- Chun, M., Toomey, D., Wahhaj, Z., Biller, B., Artigau, E., Hayward, T., Liu, M., Close, L., Hartung, M., Rigaut, F., & Ftacilas, C. 2008, in *Society of Photo-Optical Instrumentation Engineers (SPIE) Conference Series*, Vol. 7015, *Society of Photo-Optical Instrumentation Engineers (SPIE) Conference Series*
- Covey, K. R., Lada, C. J., Román-Zúñiga, C., Muench, A. A., Forbrich, J., & Ascenso, J. 2010, *ApJ*, 722, 971
- Currie, T., Burrows, A., Itoh, Y., Matsumura, S., Fukagawa, M., Apai, D., Madhusudhan, N., Hinz, P. M., Rodigas, T. J., Kasper, M., Pyo, T.-S., & Ogino, S. 2011, *ApJ*, 729, 128
- Cushing, M. C., Rayner, J. T., & Vacca, W. D. 2005, *ApJ*, 623, 1115
- Cushing, M. C., Vacca, W. D., & Rayner, J. T. 2004, *PASP*, 116, 362
- Cutri, R. M., Skrutskie, M. F., van Dyk, S., Beichman, C. A., Carpenter, J. M., Chester, T., Cambresy, L., Evans, T., Fowler, J., Gizis, J., Howard, E., Huchra, J., Jarrett, T., Kopan, E. L., Kirkpatrick, J. D., Light, R. M., Marsh, K. A., McCallon, H., Schneider, S., Stiening, R., Sykes, M., Weinberg, M., Wheaton, W. A., Wheelock, S., & Zacarias, N. 2003, 2MASS All Sky Catalog of point sources. (The IRSA 2MASS All-Sky Point Source Catalog, NASA/IPAC Infrared Science Archive. <http://irsa.ipac.caltech.edu/applications/Gator/>)
- Dupuy, T. J. & Liu, M. C. 2011, *ApJ*, 733, 122
- Eggen, O. J. 1989, *PASP*, 101, 54
- Elias, J. H., Frogel, J. A., Matthews, K., & Neugebauer, G. 1982, *AJ*, 87, 1029

- Fitzpatrick, M. J. 1993, in *Astronomical Society of the Pacific Conference Series*, Vol. 52, *Astronomical Data Analysis Software and Systems II*, ed. R. J. Hanisch, R. J. V. Brissenden, & J. Barnes, 472–+
- Ghez, A. M., Salim, S., Weinberg, N. N., Lu, J. R., Do, T., Dunn, J. K., Matthews, K., Morris, M. R., Yelda, S., Becklin, E. E., Kremenek, T., Milosavljevic, M., & Naiman, J. 2008, *ApJ*, 689, 1044
- Golimowski, D. A., Leggett, S. K., Marley, M. S., Fan, X., Geballe, T. R., Knapp, G. R., Vrba, F. J., Henden, A. A., Luginbuhl, C. B., Guetter, H. H., Munn, J. A., Canzian, B., Zheng, W., Tsvetanov, Z. I., Chiu, K., Glazebrook, K., Hoversten, E. A., Schneider, D. P., & Brinkmann, J. 2004, *AJ*, 127, 3516
- Hawley, S. L., Gizis, J. E., & Reid, I. N. 1996, *AJ*, 112, 2799
- Hinkley, S., Oppenheimer, B. R., Brenner, D., Zimmerman, N., Roberts, Jr., L. C., Parry, I. R., Soummer, R., Sivaramakrishnan, A., Simon, M., Perrin, M. D., King, D. L., Lloyd, J. P., Bouchez, A., Roberts, J. E., Dekany, R., Beichman, C., Hillenbrand, L., Burruss, R., Shao, M., & Vasisht, G. 2010, *ApJ*, 712, 421
- Holman, M. J. & Wiegert, P. A. 1999, *AJ*, 117, 621
- Huélamo, N., Nürnberger, D. E. A., Ivanov, V. D., Chauvin, G., Carraro, G., Sterzik, M. F., Melo, C. H. F., Bonnefoy, M., Hartung, M., Haubois, X., & Foellmi, C. 2010, *A&A*, 521, L54
- Johnson, J. A., Aller, K. M., Howard, A. W., & Crepp, J. R. 2010, *PASP*, 122, 905
- Johnson, J. A., Gazak, J. Z., Apps, K., Muirhead, P. S., Crepp, J. R., Crossfield, I. J. M., Boyajian, T., von Braun, K., Rojas-Ayala, B., Howard, A. W., Covey, K. R., Schlawin, E., Hamren, K., Morton, T. D., & Lloyd, J. P. 2011, *ArXiv e-prints*
- Jura, M., Malkan, M., White, R., Telesco, C., Pina, R., & Fisher, R. S. 1998, *ApJ*, 505, 897
- Kalas, P., Graham, J. R., Chiang, E., Fitzgerald, M. P., Clampin, M., Kite, E. S., Stapelfeldt, K., Marois, C., & Krist, J. 2008, *Science*, 322, 1345
- Kelson, D. D. 2003, *PASP*, 115, 688
- Kraus, A. L. & Hillenbrand, L. A. 2008, *ApJ*, 686, L111
- . 2009, *ApJ*, 704, 531
- Kraus, A. L. & Ireland, M. J. 2012, *ApJ*, 745, 5
- Kraus, A. L., Ireland, M. J., Hillenbrand, L. A., & Martinache, F. 2012, *ApJ*, 745, 19
- Kraus, A. L., Ireland, M. J., Martinache, F., & Hillenbrand, L. A. 2011, *ApJ*, 731, 8

- Lafrenière, D., Doyon, R., Marois, C., Nadeau, D., Oppenheimer, B. R., Roche, P. F., Rigaut, F., Graham, J. R., Jayawardhana, R., Johnstone, D., Kalas, P. G., Macintosh, B., & Racine, R. 2007, *ApJ*, 670, 1367
- Lafrenière, D., Jayawardhana, R., & van Kerkwijk, M. H. 2008, *ApJ*, 689, L153
- Lagrange, A.-M., Gratadour, D., Chauvin, G., Fusco, T., Ehrenreich, D., Mouillet, D., Rousset, G., Rouan, D., Allard, F., Gendron, É., Charton, J., Mugnier, L., Rabou, P., Montri, J., & Lacombe, F. 2009, *A&A*, 493, L21
- Leggett, S. K., Allard, F., Dahn, C., Hauschildt, P. H., Kerr, T. H., & Rayner, J. 2000, *ApJ*, 535, 965
- Leggett, S. K., Burningham, B., Saumon, D., Marley, M. S., Warren, S. J., Smart, R. L., Jones, H. R. A., Lucas, P. W., Pinfield, D. J., & Tamura, M. 2010, *ApJ*, 710, 1627
- Leggett, S. K., Currie, M. J., Varricatt, W. P., Hawarden, T. G., Adamson, A. J., Buckle, J., Carroll, T., Davies, J. K., Davis, C. J., Kerr, T. H., Kuhn, O. P., Seigar, M. S., & Wold, T. 2006, *MNRAS*, 373, 781
- Leggett, S. K., Hawarden, T. G., Currie, M. J., Adamson, A. J., Carroll, T. C., Kerr, T. H., Kuhn, O. P., Seigar, M. S., Varricatt, W. P., & Wold, T. 2003, *MNRAS*, 345, 144
- Liu, M. C. 2004, *Science*, 305, 1442
- Liu, M. C., Dupuy, T. J., & Leggett, S. K. 2010a, *ApJ*, 722, 311
- Liu, M. C., Wahhaj, Z., Biller, B. A., Nielsen, E. L., Chun, M., Close, L. M., Ftaclos, C., Hartung, M., Hayward, T. L., Clarke, F., Reid, I. N., Shkolnik, E. L., Tecza, M., Thatte, N., Alencar, S., Artymowicz, P., Boss, A., Burrows, A., de Gouveia Dal Pino, E., Gregorio-Hetem, J., Ida, S., Kuchner, M. J., Lin, D., & Toomey, D. 2010b, in *Society of Photo-Optical Instrumentation Engineers (SPIE) Conference Series*, Vol. 7736, *Society of Photo-Optical Instrumentation Engineers (SPIE) Conference Series*
- Lowrance, P. J., McCarthy, C., Becklin, E. E., Zuckerman, B., Schneider, G., Webb, R. A., Hines, D. C., Kirkpatrick, J. D., Koerner, D. W., Low, F., Meier, R., Rieke, M., Smith, B. A., Terrile, R. J., & Thompson, R. I. 1999, *ApJ*, 512, L69
- Lowrance, P. J., Schneider, G., Kirkpatrick, J. D., Becklin, E. E., Weinberger, A. J., Zuckerman, B., Plait, P., Malmuth, E. M., Heap, S. R., Schultz, A., Smith, B. A., Terrile, R. J., & Hines, D. C. 2000, *ApJ*, 541, 390
- Luhman, K. L. 1999, *ApJ*, 525, 466
- Luhman, K. L., Allen, P. R., Espaillat, C., Hartmann, L., & Calvet, N. 2010, *ApJS*, 186, 111
- Luhman, K. L., Mamajek, E. E., Allen, P. R., & Cruz, K. L. 2009, *ApJ*, 703, 399

- Marcy, G. W., Butler, R. P., Vogt, S. S., Fischer, D. A., Wright, J. T., Johnson, J. A., Tinney, C. G., Jones, H. R. A., Carter, B. D., Bailey, J., O’Toole, S. J., & Upadhyay, S. 2008, *Physica Scripta Volume T*, 130, 014001
- Marois, C., Lafrenière, D., Doyon, R., Macintosh, B., & Nadeau, D. 2006, *ApJ*, 641, 556
- Marois, C., Macintosh, B., Barman, T., Zuckerman, B., Song, I., Patience, J., Lafrenière, D., & Doyon, R. 2008, *Science*, 322, 1348
- Marois, C., Zuckerman, B., Konopacky, Q. M., Macintosh, B., & Barman, T. 2010, *Nature*, 468, 1080
- Mayor, M., Udry, S., Lovis, C., Pepe, F., Queloz, D., Benz, W., Bertaux, J.-L., Bouchy, F., Mordasini, C., & Segransan, D. 2009, *A&A*, 493, 639
- McGovern, M. R., Kirkpatrick, J. D., McLean, I. S., Burgasser, A. J., Prato, L., & Lowrance, P. J. 2004, *ApJ*, 600, 1020
- Merín, B., Montesinos, B., Eiroa, C., Solano, E., Mora, A., D’Alessio, P., Calvet, N., Oudmaijer, R. D., de Winter, D., Davies, J. K., Harris, A. W., Collier Cameron, A., Deeg, H. J., Ferlet, R., Garzón, F., Grady, C. A., Horne, K., Miranda, L. F., Palacios, J., Penny, A., Quirrenbach, A., Rauer, H., Schneider, J., & Wesselius, P. R. 2004, *A&A*, 419, 301
- Mohanty, S., Jayawardhana, R., Huélamo, N., & Mamajek, E. 2007, *ApJ*, 657, 1064
- Nidever, D. L., Marcy, G. W., Butler, R. P., Fischer, D. A., & Vogt, S. S. 2002, *ApJS*, 141, 503
- Nielsen, E. L. & Close, L. M. 2010, *ApJ*, 717, 878
- Nielsen, E. L., Close, L. M., Biller, B. A., Masciadri, E., & Lenzen, R. 2008, *ApJ*, 674, 466
- Pedicelli, S., Bono, G., Lemasle, B., François, P., Groenewegen, M., Lub, J., Pel, J. W., Laney, D., Piersimoni, A., Romaniello, M., Buonanno, R., Caputo, F., Cassisi, S., Castelli, F., Leurini, S., Pietrinferni, A., Primas, F., & Pritchard, J. 2009, *A&A*, 504, 81
- Racine, R., Walker, G. A. H., Nadeau, D., Doyon, R., & Marois, C. 1999, *PASP*, 111, 587
- Raghavan, D., McAlister, H. A., Henry, T. J., Latham, D. W., Marcy, G. W., Mason, B. D., Gies, D. R., White, R. J., & ten Brummelaar, T. A. 2010, *ApJS*, 190, 1
- Rayner, J. T., Cushing, M. C., & Vacca, W. D. 2009, *ApJS*, 185, 289
- Rayner, J. T., Toomey, D. W., Onaka, P. M., Denault, A. J., Stahlberger, W. E., Watanabe, D. Y., & Wang, S.-I. 1998, in *Society of Photo-Optical Instrumentation Engineers (SPIE) Conference Series*, Vol. 3354, Society of Photo-Optical Instrumentation Engineers (SPIE) Conference Series, ed. A. M. Fowler, 468–479

- Rebolo, R., Zapatero Osorio, M. R., Madrugá, S., Bejar, V. J. S., Arribas, S., & Licandro, J. 1998, *Science*, 282, 1309
- Rojas-Ayala, B., Covey, K. R., Muirhead, P. S., & Lloyd, J. P. 2010, *ApJ*, 720, L113
- Röser, S., Schilbach, E., Piskunov, A. E., Kharchenko, N. V., & Scholz, R.-D. 2011, *A&A*, 531, A92+
- Schlegel, D. J., Finkbeiner, D. P., & Davis, M. 1998, *ApJ*, 500, 525
- Siess, L., Dufour, E., & Forestini, M. 2000, *A&A*, 358, 593
- Soderblom, D. R. 2010, *ARA&A*, 48, 581
- Stauffer, J. R., Hartmann, L. W., Fazio, G. G., Allen, L. E., Patten, B. M., Lowrance, P. J., Hurt, R. L., Rebull, L. M., Cutri, R. M., Ramirez, S. V., Young, E. T., Rieke, G. H., Gorlova, N. I., Muzerolle, J. C., Slesnick, C. L., & Skrutskie, M. F. 2007, *ApJS*, 172, 663
- Su, K. Y. L., Rieke, G. H., Stansberry, J. A., Bryden, G., Stapelfeldt, K. R., Trilling, D. E., Muzerolle, J., Beichman, C. A., Moro-Martin, A., Hines, D. C., & Werner, M. W. 2006, *ApJ*, 653, 675
- Toomey, D. W. & Ftaclas, C. 2003, in *Society of Photo-Optical Instrumentation Engineers (SPIE) Conference Series*, Vol. 4841, *Society of Photo-Optical Instrumentation Engineers (SPIE) Conference Series*, ed. M. Iye & A. F. M. Moorwood, 889–900
- Torres, C. A. O., Quast, G. R., Melo, C. H. F., & Sterzik, M. F. 2008, *Handbook of Star Forming Regions*, Volume II, 757
- Vacca, W. D., Cushing, M. C., & Rayner, J. T. 2003, *PASP*, 115, 389
- van Leeuwen, F. 2007, *A&A*, 474, 653
- Wahhaj, Z., Liu, M. C., Biller, B. A., Clarke, F., Nielsen, E. L., Close, L. M., Hayward, T. L., Mamajek, E. E., Cushing, M., Dupuy, T., Tecza, M., Thatte, N., Chun, M., Ftaclas, C., Hartung, M., Reid, I. N., Shkolnik, E. L., Alencar, S. H. P., Artymowicz, P., Boss, A., de Gouveia Dal Pino, E., Gregorio-Hetem, J., Ida, S., Kuchner, M., Lin, D. N. C., & Toomey, D. W. 2011, *ApJ*, 729, 139

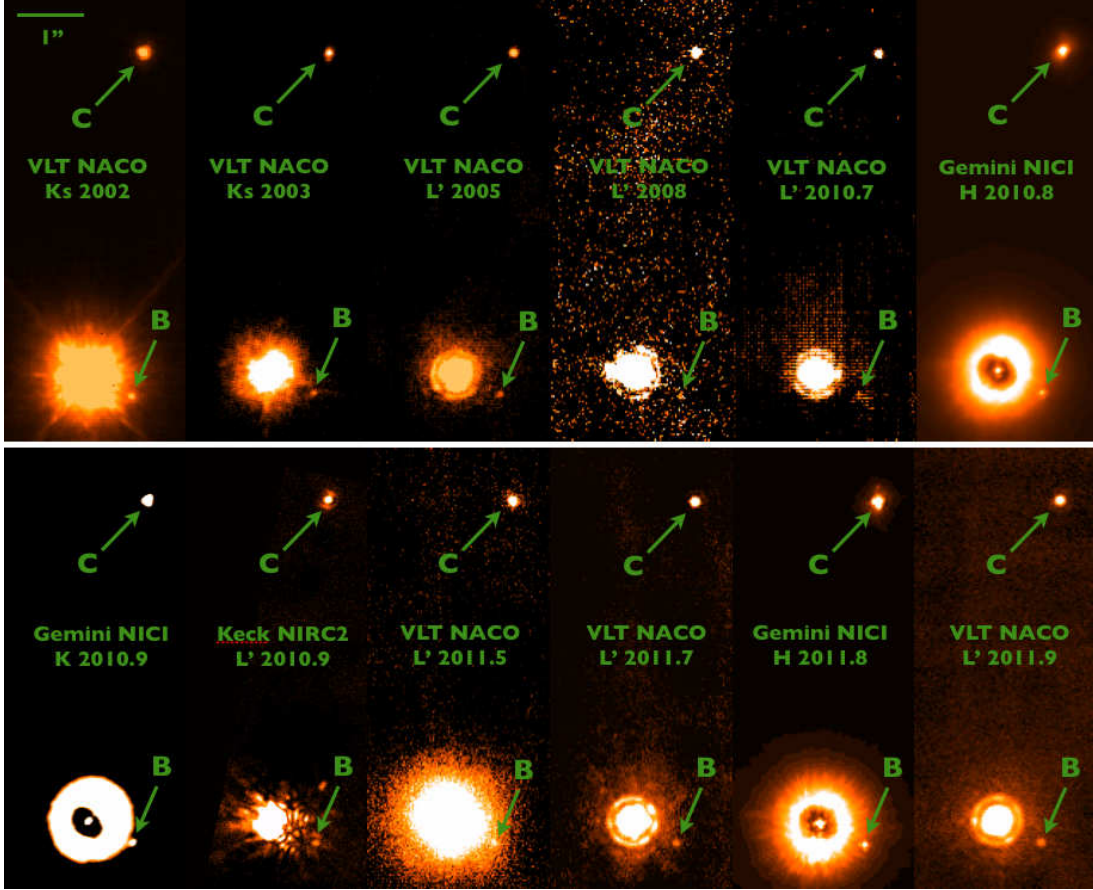


Fig. 1.— Images of HD 1160 A, B, and C over twelve epochs from 2002 to late 2011. The VLT NACO data were taken as calibration data for science programs targeting other objects, and in some cases HD 1160 B is detected at low S/N. Each image was rotated to place North up and East to the left and has the same field of view, $2.7'' \times 6.5''$.

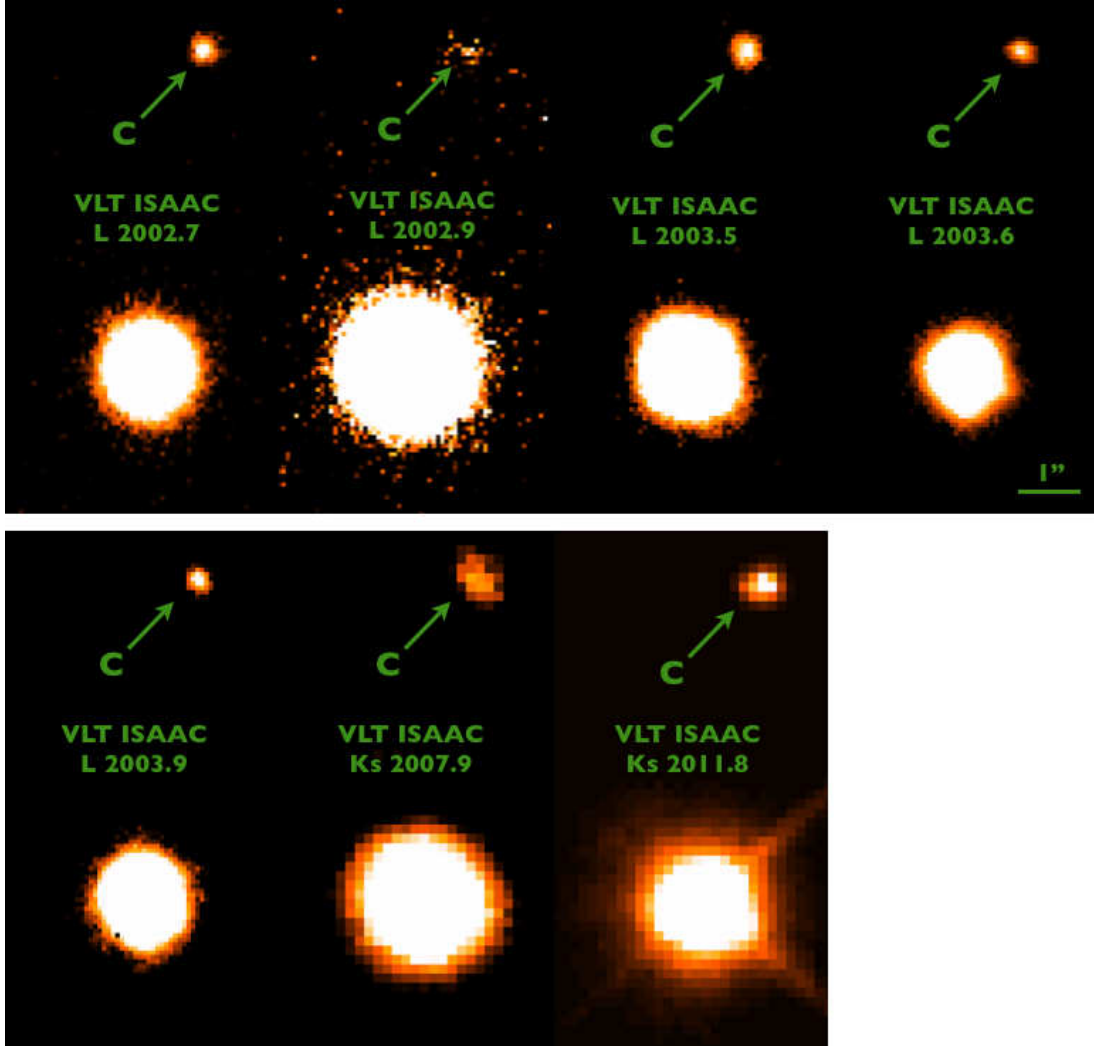


Fig. 2.— Archival images of HD 1160 A and C from 2002 until 2011, taken with the VLT ISAAC instrument. As with the VLT NACO data, these are calibration data and are sometimes at low S/N. Additionally, since the seeing-limited resolution of ISAAC is lower than the AO-corrected images in Figure 1, HD 1160 B is not detected at any of these epochs. Each image was rotated to place North up and East to the left and has the same field of view, $2.7'' \times 6.5''$.

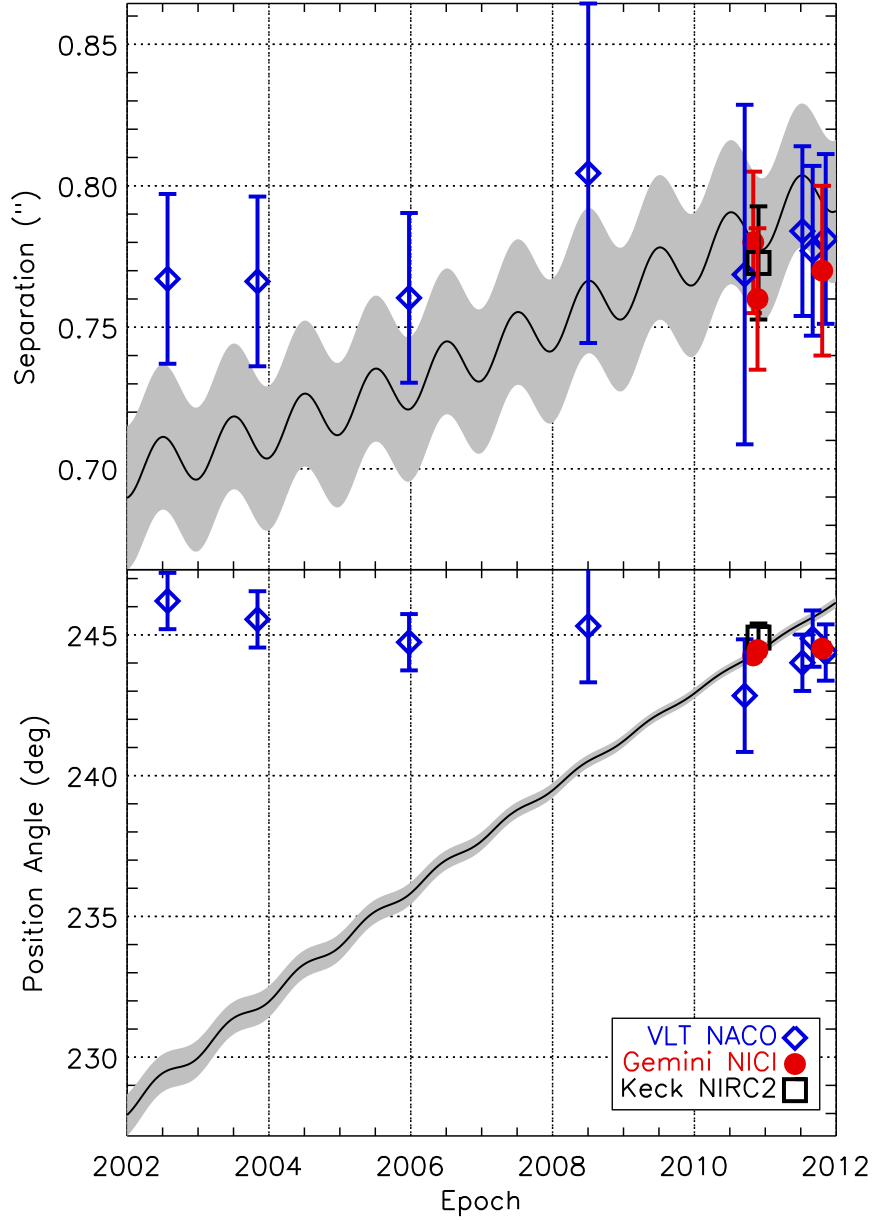


Fig. 3.— Astrometry of HD 1160 B from 2002 to 2011 (points with error bars) along with the expected motion of a background object (black line). A background object should fall within the gray shaded track, given the known proper motion and parallax of HD 1160 A. The thickness of the gray track indicates the positional uncertainties arising from the proper motion and parallax uncertainties for HD 1160 A, as well as the astrometric uncertainties from the NIRC2 2010.8301 position to which the track is tied. HD 1160 B is clearly a common proper motion companion.

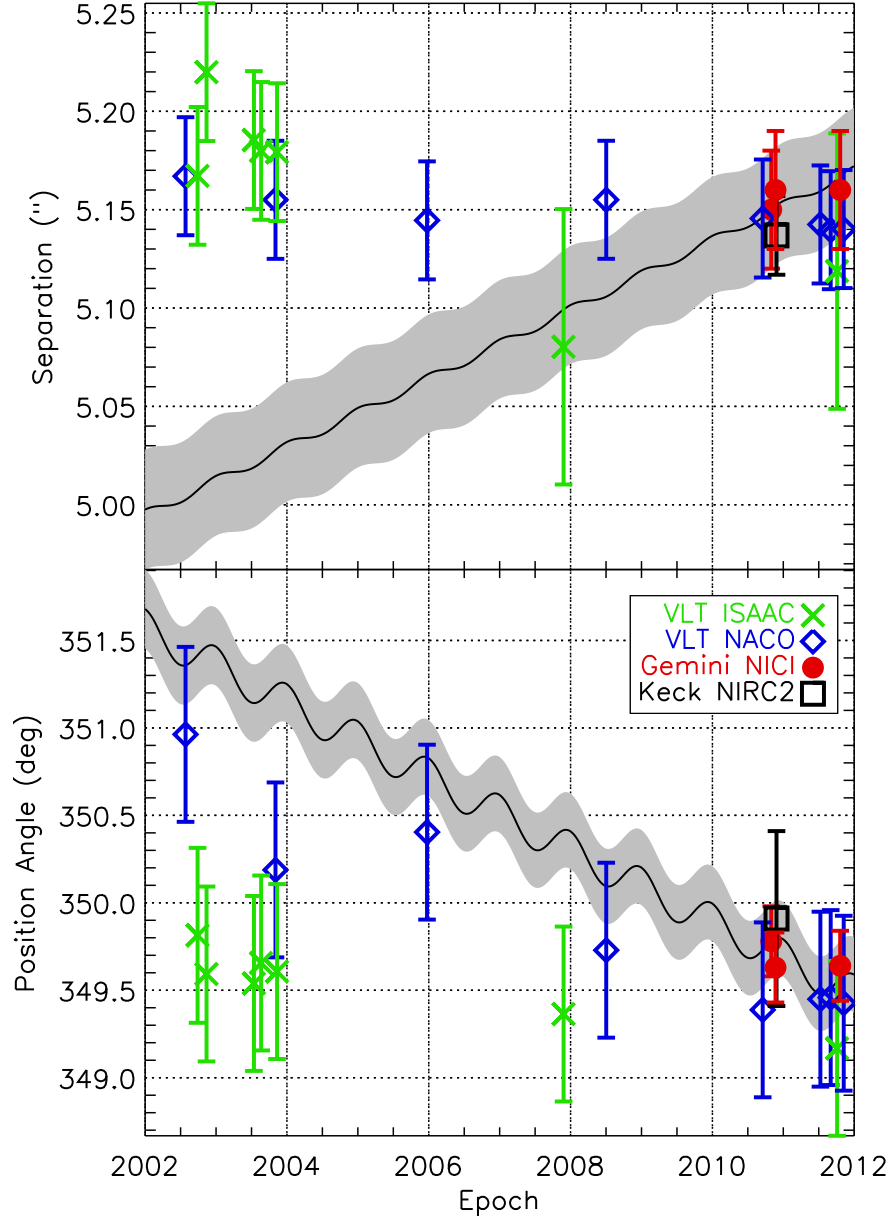


Fig. 4.— Astrometry of HD 1160 C from 2002 to 2011. While a less significant detection of common proper motion than with HD 1160 B, the data are still much more consistent with HD 1160 C being a co-moving companion rather than a distant background object.

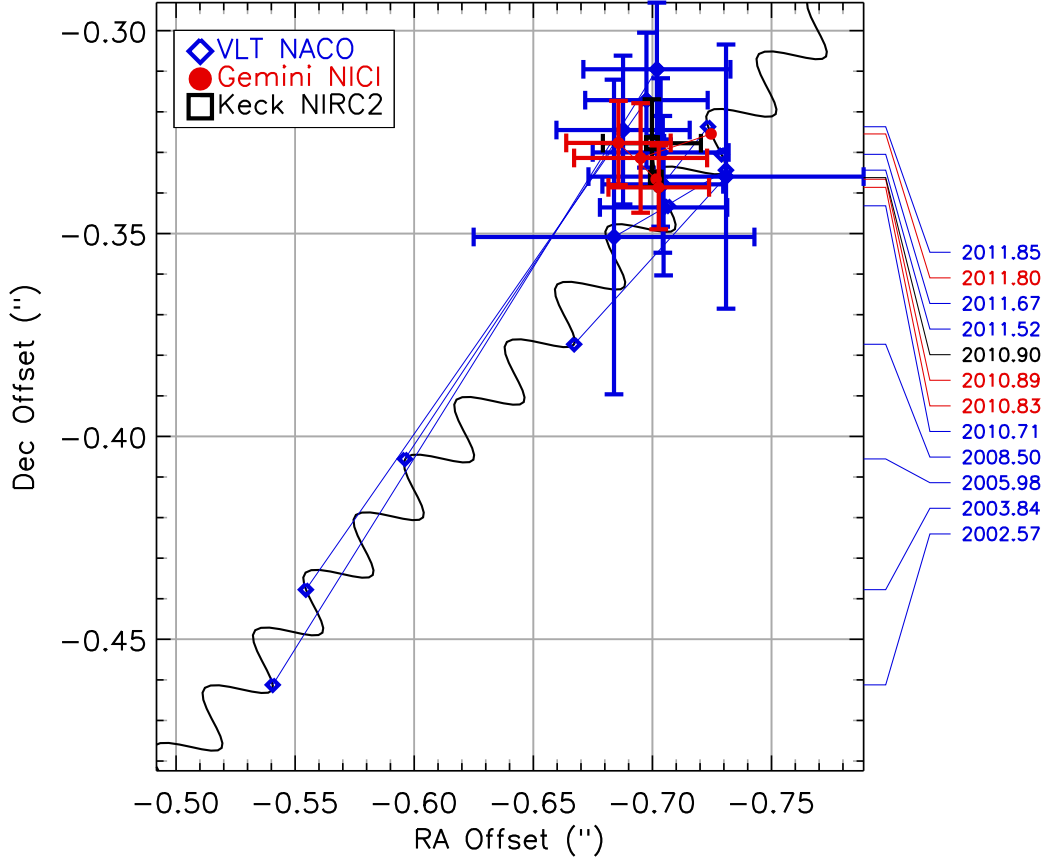


Fig. 5.— Astrometry for HD 1160 B with respect to HD 1160 A as seen on the sky. Each data point is connected by a thin line to the expected location of a distant background object at the observational epoch. The labels on the right give the epoch of the astrometric measurements, with the vertical location of the epoch label set by the Declination expected for a distant background object at the epoch. Within the error bars, all the datapoints are consistent with the position measured at the NICI 2010.8301 detection and are significantly displaced from the expected positions for a distant background object. The reduced χ^2 value for HD 1160 B being a background object is 26.2 (dof=22, $P \approx 0\%$), compared to $\chi^2_{\nu} = 0.38$ (dof=22, $P = 99.6\%$) for a common proper motion companion.

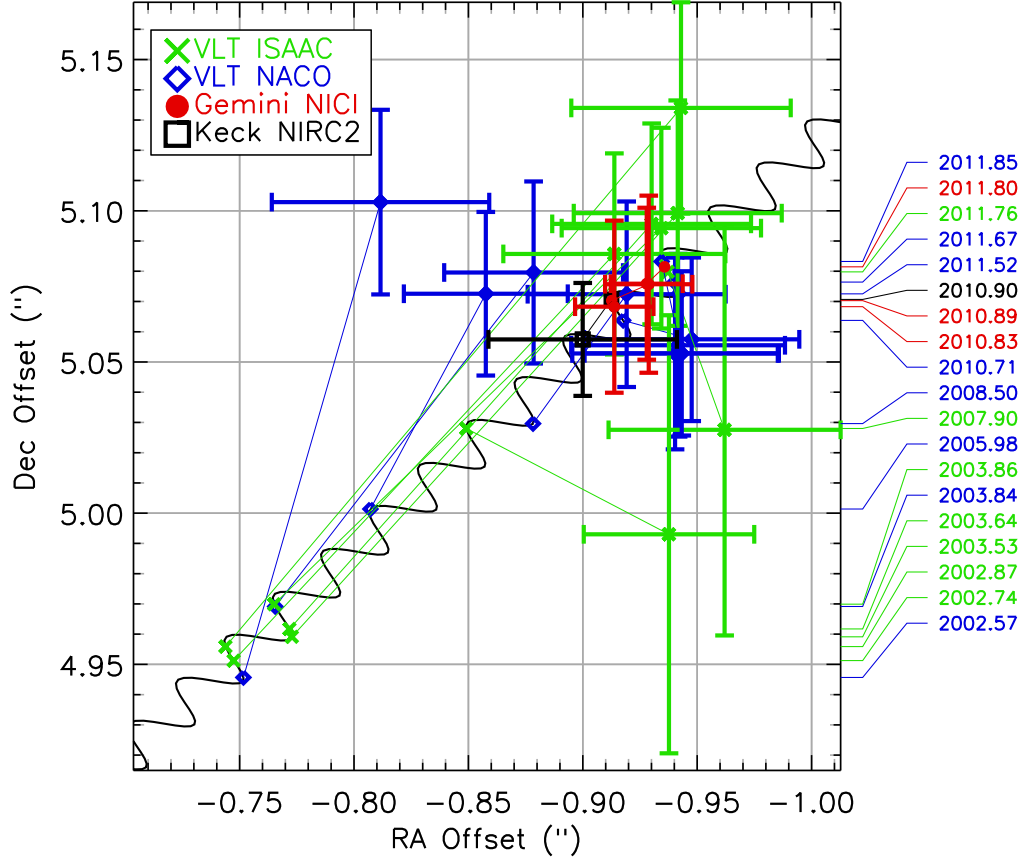


Fig. 6.— On-sky astrometric plot for HD 1160 C with respect to HD 1160 A. The fit to the motion of a common proper motion companion is much more likely than the fit to the motion of a background object: the significance of the fit is $\chi^2_\nu = 4.95$ (dof=36 $P \approx 0\%$) for a background object and $\chi^2_\nu = 0.62$ (dof = 36, $P=96.5\%$) for a common proper motion companion. In addition, the expected direction of the motion of a background object is orthogonal to the spread of the datapoints, and we have measured the radial velocities of HD 1160 A and C to be consistent within measurement uncertainty.

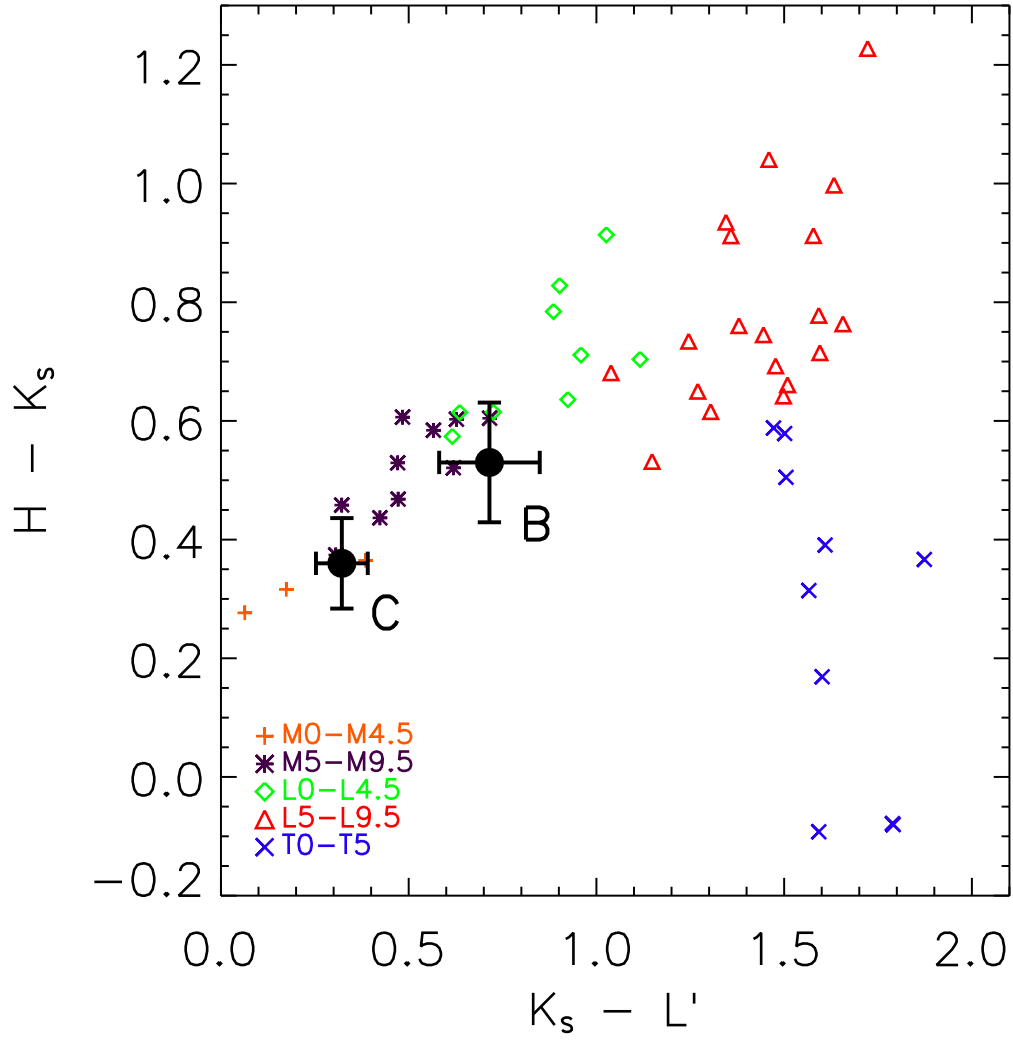


Fig. 7.— Color-color diagram on the MKO system, suggesting spectral types of early-L and mid-M for HD 1160 B and C, respectively. The low-mass field dwarfs plotted here are from the compilation of Leggett et al. (2010). The implied spectral type for HD 1160 C is a close match to our determination of M3.5 based on near-IR spectroscopy.

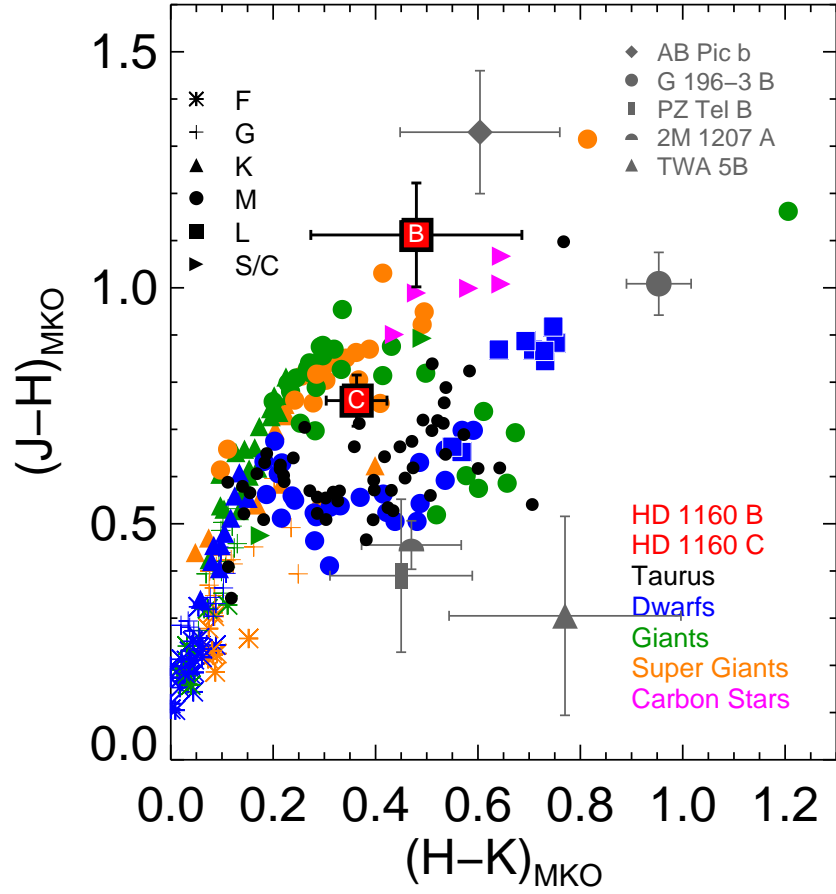


Fig. 8.— Color-color diagram showing HD 1160 B and C, along with giants, dwarfs, single-star members of Taurus, and some individual low-mass objects. While HD 1160 B and C are not giants themselves, they do exhibit giant-like JHK colors.

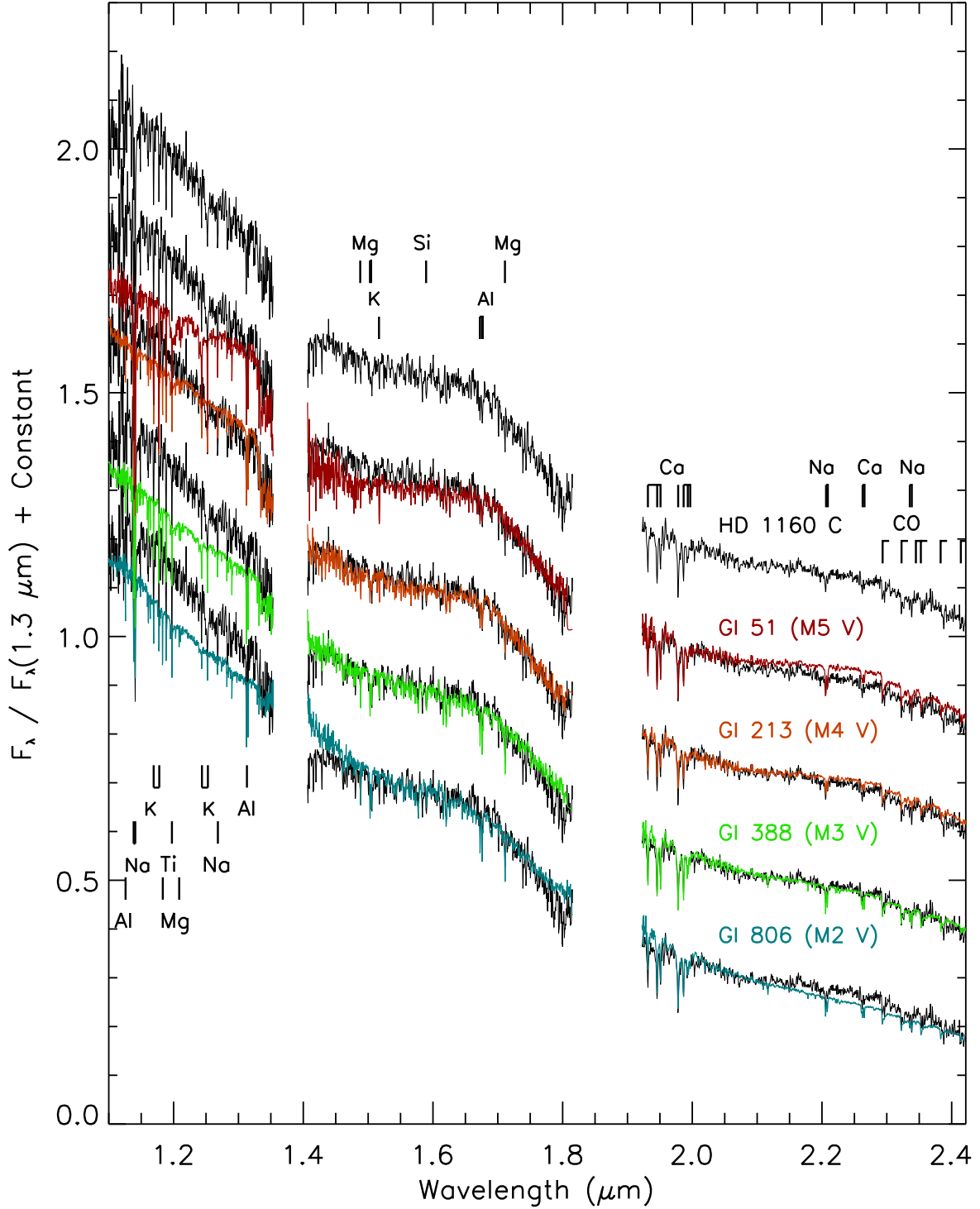


Fig. 9.— IRTF/SpEx spectra of HD 1160 C compared to M dwarf spectral standards and line identifications from Cushing et al. (2005). The best fits to the shape of the H and K continuum are spectral types M3 and M4, and therefore we assign a spectral type of M3.5. Note that the J -band portion of the spectrum suffers from contamination from HD 1160 A (A0), and so we only use the H and K portions in our fits.

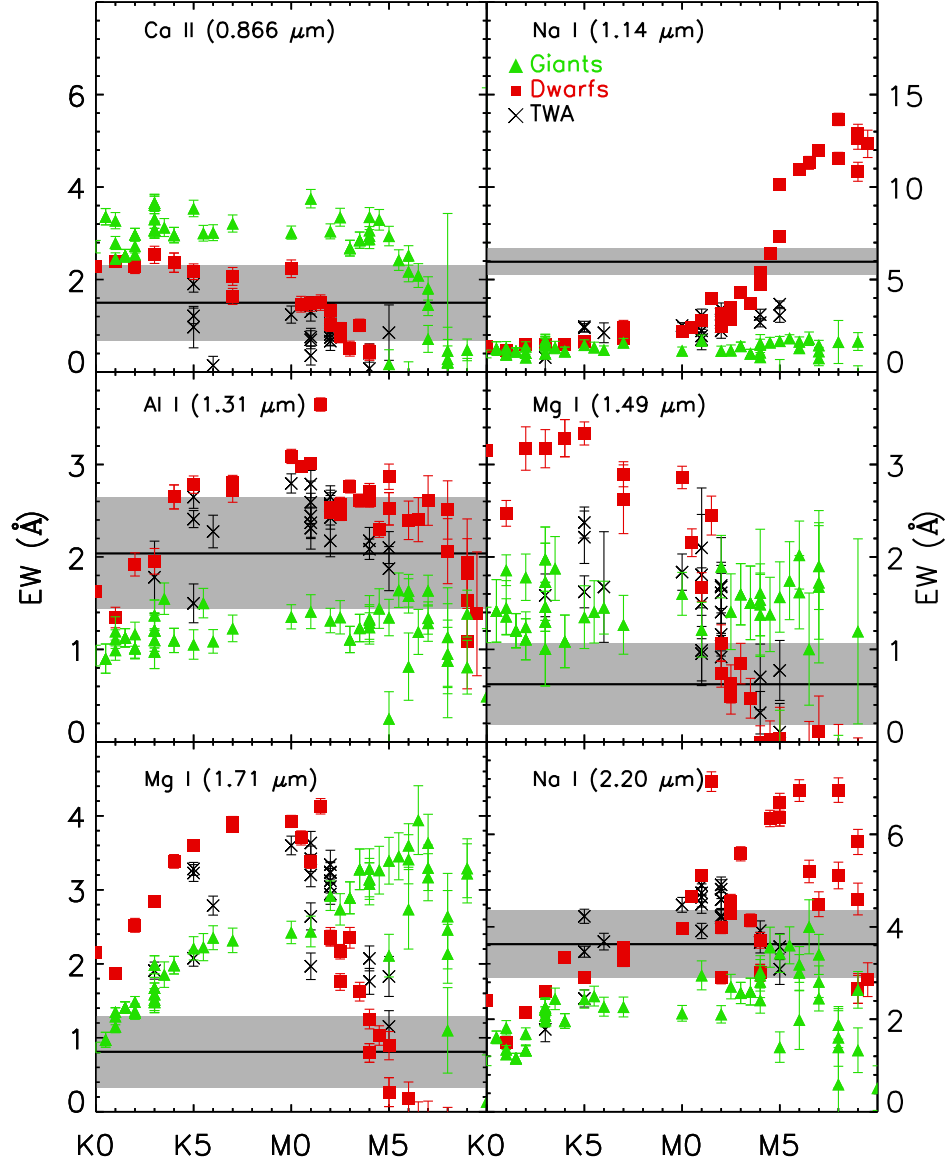


Fig. 10.— Comparison of equivalent widths of atomic features in the HD 1160 C spectrum to those of dwarf and giant stars from Rayner et al. (2009) and members of the TW Hydra Association (TWA) from Covey et al. (2010). Red squares denote dwarfs, green triangles giants, and black crosses TWA members. For each feature, the black horizontal line denotes the equivalent width of HD 1160 C and the gray swath the corresponding measurement uncertainty. Taken together, the atomic absorption lines support our M3.5 spectral type for HD 1160 C. However, these data cannot constrain the age of HD 1160 C, since the equivalent widths for M dwarfs and TWA members are similar.

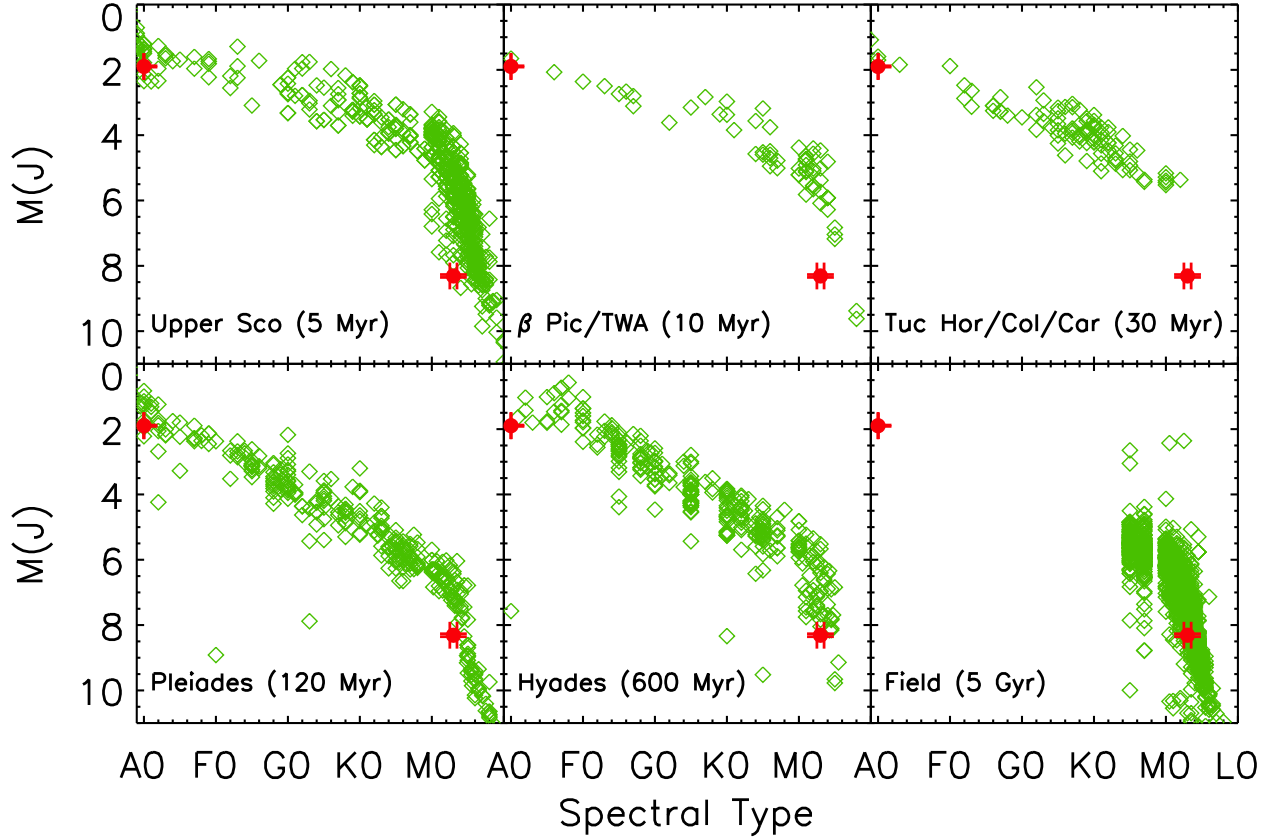


Fig. 11.— HR diagram of stars in Upper Sco, 10 Myr moving groups (β Pic and TW Hya), 30 Myr moving groups (Tuc/Hor, Carina, and Columba), the Pleiades, the Hyades, and field low-mass objects (magnitudes are in the 2MASS system). The positions of HD 1160 A and C are marked with filled red circles. We do not include HD 1160 B, as we do not have a spectral type. HD 1160 A appears underluminous compared to other A stars, especially for older stars in the Hyades.

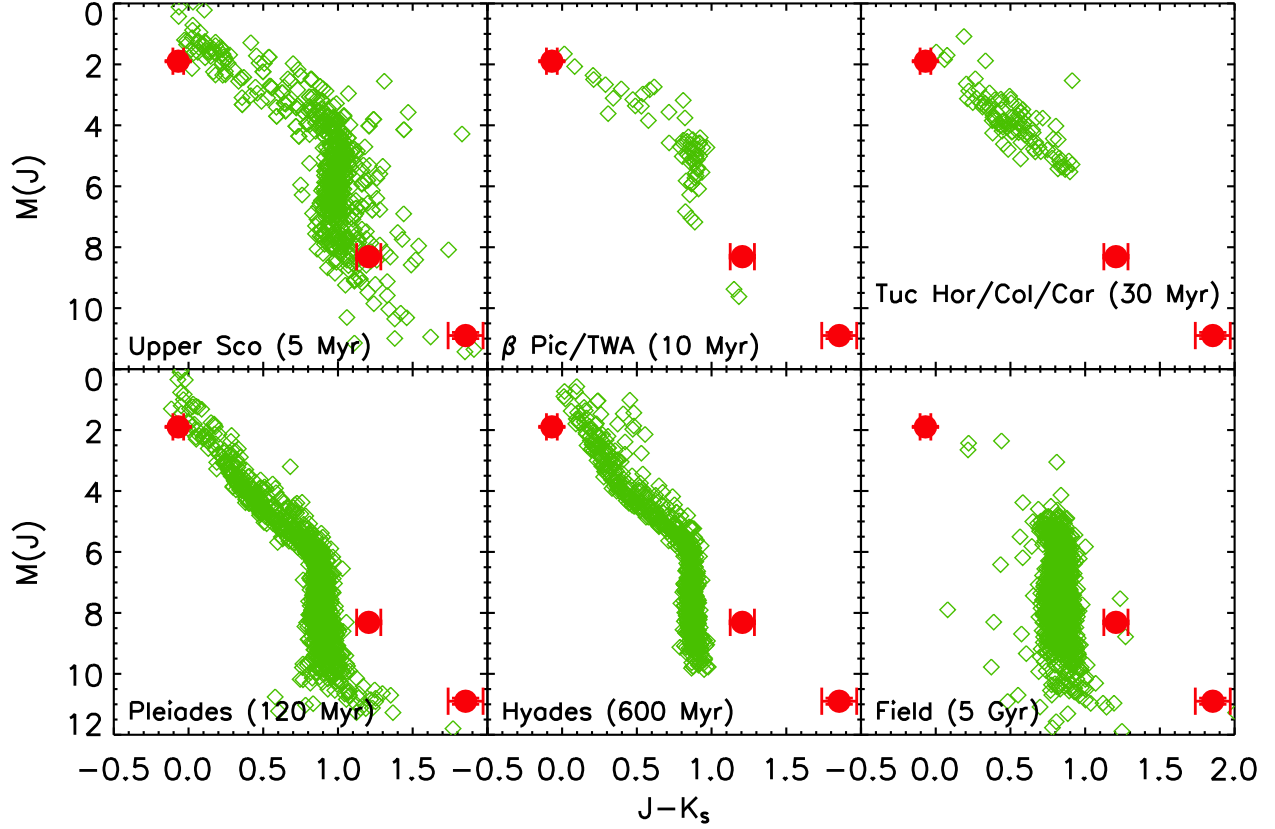


Fig. 12.— Color-magnitude diagram (2MASS system) showing HD 1160 ABC with respect to stars in stellar associations of different ages. HD 1160 A is too underluminous to fit either the Hyades or Pleiades stars, while HD 1160 B and C are too red to fit the low-mass end of the main sequence of these older open clusters or field objects. The HD 1160 system does appear consistent with the stars in Upper Sco and the 10 and 30 Myr moving groups. As a result, we assign an age to the system of 50^{+50}_{-40} Myr.

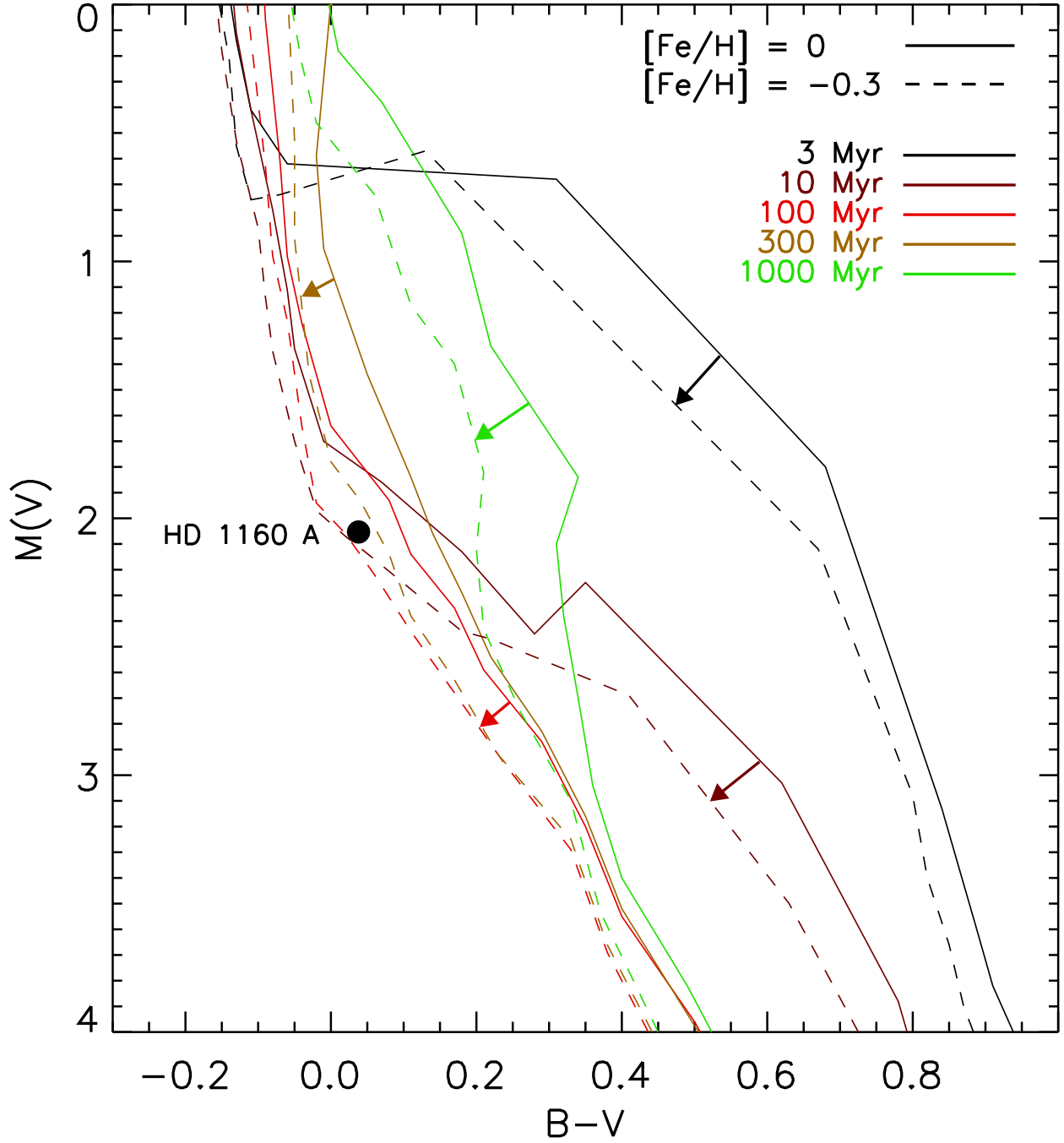


Fig. 13.— Optical color-magnitude diagram showing the position of HD 1160 A (filled circle) against Siess et al. (2000) isochrones, for solar metallicity (solid lines) and half-solar abundance (dashed). HD 1160 A is underluminous compared to tracks of all ages at $[Fe/H] = 0.0$, but is consistent with ages of 10–300 Myr for $[Fe/H] = -0.3$. However, the colors of the B and C components do not agree with a low metallicity for the system (see Figure 14)

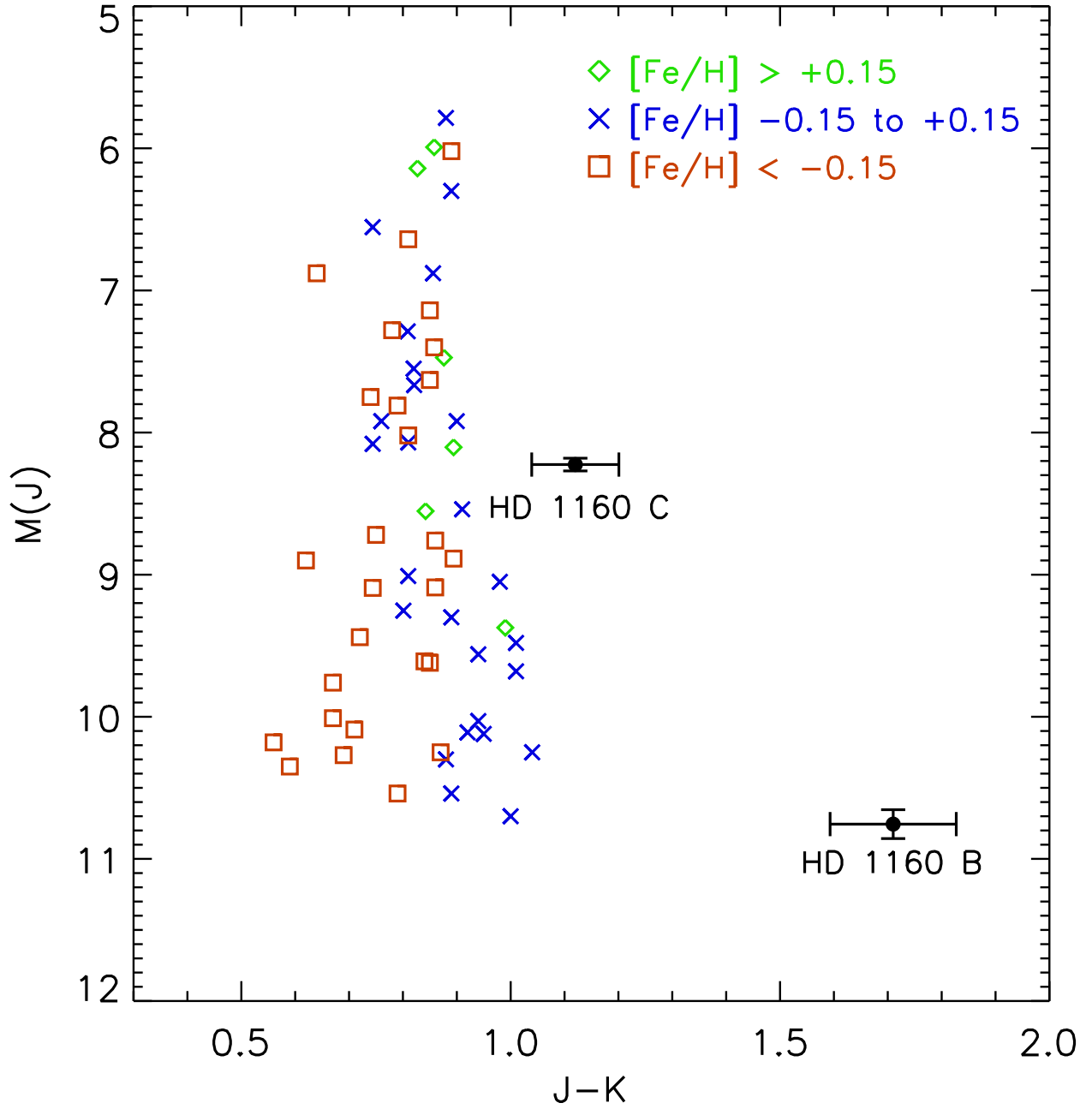


Fig. 14.— HD 1160 B and C compared to M dwarfs of known metallicity, compiled by Rojas-Ayala et al. (2010) and Leggett et al. (2000). Low-metallicity M dwarfs tend to be bluer in $J - K$ color than solar-metallicity dwarfs, especially at later spectral types. So while the under-luminosity of A stars such as HD 1160 A can be explained by either youth or sub-solar metallicity, the $J - K$ redness of HD 1160 B and C supports the idea that the system is young.

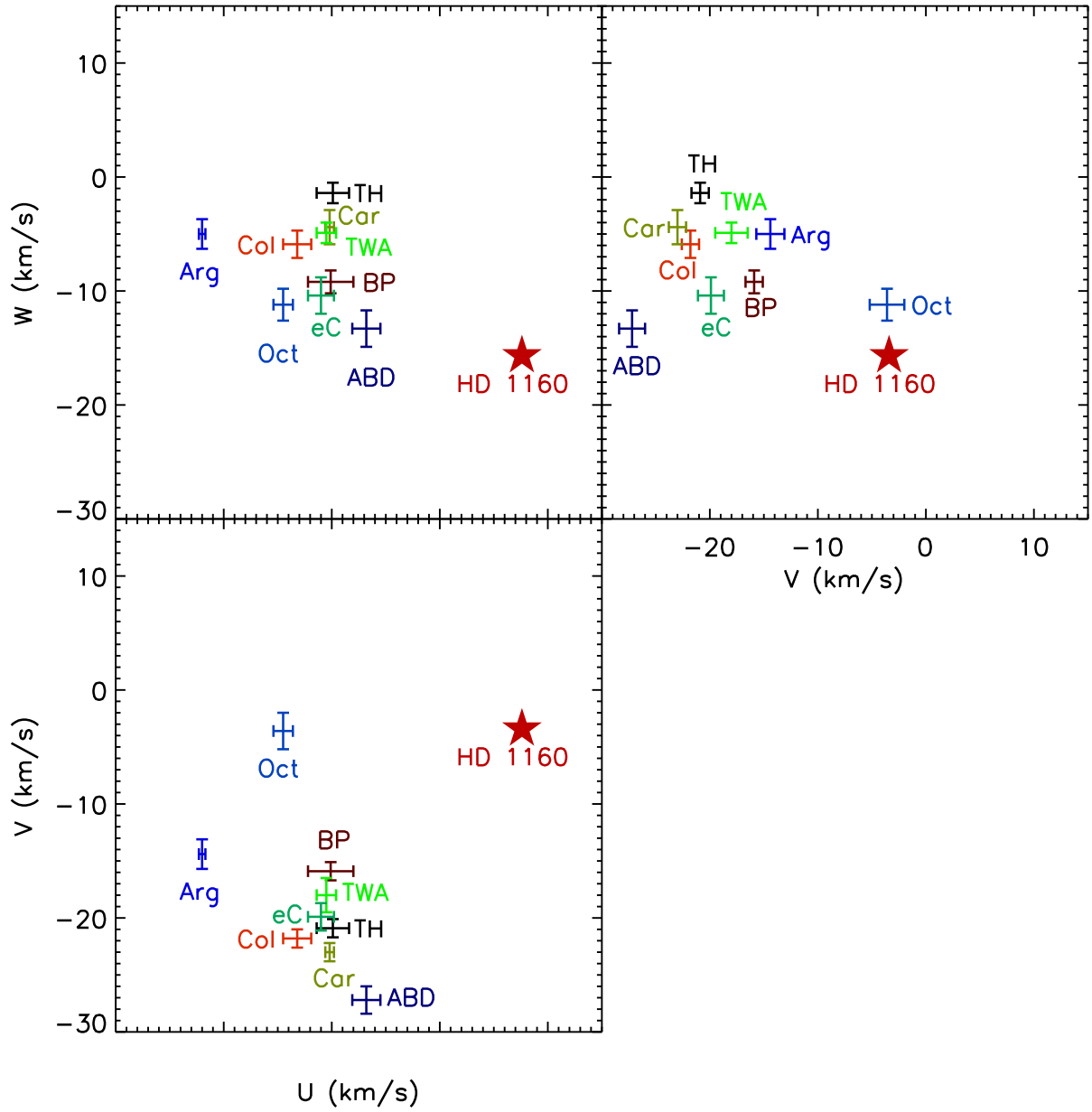


Fig. 15.— UVW motions of nearby young, moving groups from Torres et al. (2008) compared to the HD 1160 system (BP: β Pic, TH: Tuc/Hor, Col: Columba, Car: Carina, TWA: TW Hya, eC: η Cha, Oct: Octans, Arg: Argus, ABD: AB Dor). Error bars for the moving groups indicate the RMS of the space motions for the association members, while the error bars for HD 1160 indicate measurement uncertainties. HD 1160 is not co-moving with any well-known association, though the magnitude of its space motion is consistent with these young stars, supporting a young age (<100 Myr) for HD 1160.

Table 1. Properties of HD 1160 A

Property	Measurement
Spectral Type	A0V
RA (ep J2000)	00:15:57.3025
Dec (ep J2000)	+04:15:04.018
Proper Motion RA (mas/yr)	21.15 ± 0.62 ^a
Proper Motion Dec (mas/yr)	-14.20 ± 0.24 ^a
Parallax (mas)	9.66 ± 0.45 ^a
Radial Velocity (km/s)	12.6 ± 0.3 ^b
U (km/s)	7.6 ± 0.4 ^b
V (km/s)	-3.4 ± 0.5 ^b
W (km/s)	-15.7 ± 0.4 ^b
J (mag)	6.98 ± 0.02 ^c
H (mag)	7.01 ± 0.02 ^c
K_S (mag)	7.04 ± 0.03 ^c
L' (mag)	7.055 ± 0.014 ^d
M_S (mag)	7.04 ± 0.02 ^d
Age (Myr)	50^{+50}_{-40} ^b

^avan Leeuwen (2007)

^bThis work

^cCutri et al. (2003)

^dLeggett et al. (2003)

Table 2. Astrometry of HD 1160 BC

Epoch	HD 1160 B		HD 1160 C		Instrument
	Sep (″)	PA (°)	Sep (″)	PA (°)	
2002.5699	0.77 ± 0.03	246.2 ± 1.0	5.17 ± 0.03	350.9 ± 0.5	VLT NACO K_S
2002.7397	5.17 ± 0.04	349.8 ± 0.5	VLT ISAAC L
2002.8658	5.22 ± 0.04	349.6 ± 0.5	VLT ISAAC L
2003.5342	5.19 ± 0.04	349.5 ± 0.5	VLT ISAAC L
2003.6356	5.18 ± 0.04	349.7 ± 0.5	VLT ISAAC L
2003.8384	0.77 ± 0.03	245.6 ± 1.0	5.16 ± 0.03	350.1 ± 0.5	VLT NACO K_S
2003.8603	5.18 ± 0.04	349.6 ± 0.5	VLT ISAAC L
2005.9753	0.76 ± 0.03	244.7 ± 1.0	5.15 ± 0.03	350.4 ± 0.5	VLT NACO L'
2007.9014	5.08 ± 0.07	349.4 ± 0.5	VLT ISAAC K_s
2008.5027	0.80 ± 0.06	245.3 ± 2	5.16 ± 0.03	349.7 ± 0.5	VLT NACO L'
2010.7096	0.77 ± 0.06	242.8 ± 2	5.15 ± 0.03	349.4 ± 0.5	VLT NACO L'
2010.8301	0.78 ± 0.03	244.3 ± 0.2	5.15 ± 0.03	349.8 ± 0.2	Gemini NICI H
2010.8904	0.76 ± 0.03	244.5 ± 0.2	5.16 ± 0.03	349.6 ± 0.2	Gemini NICI H
2010.9041	0.78 ± 0.02	244.9 ± 0.5	5.14 ± 0.02	349.9 ± 0.5	Keck NIRC2 L'
2011.5233	0.78 ± 0.03	244.0 ± 1.0	5.14 ± 0.03	349.4 ± 0.5	VLT NACO L'
2011.6685	0.78 ± 0.03	244.9 ± 1.0	5.14 ± 0.03	349.5 ± 0.5	VLT NACO L'
2011.7589	5.12 ± 0.07	349.2 ± 0.5	VLT ISAAC K_s
2011.8027	0.77 ± 0.03	244.5 ± 0.2	5.16 ± 0.03	349.6 ± 0.2	Gemini NICI H
2011.8521	0.78 ± 0.03	244.4 ± 1.0	5.14 ± 0.03	349.4 ± 0.5	VLT NACO L'

Table 3. Photometry of HD 1160 BC

Bandpass (MKO)	HD 1160 B (mag)	HD 1160 C (mag)	Instrument
ΔJ	8.85 ± 0.10	6.33 ± 0.04	Gemini NICI
ΔH	7.64 ± 0.08	5.53 ± 0.03	Gemini NICI
ΔK_S	7.08 ± 0.05	5.14 ± 0.06	Gemini NICI
$\Delta L'$	6.35 ± 0.12	4.803 ± 0.005	Keck NIRC2
ΔM_S	7.3 ± 0.2	5.10 ± 0.05	Keck NIRC2
M_J	10.75 ± 0.10	8.23 ± 0.04	
M_H	9.57 ± 0.08	7.46 ± 0.04	
M_{K_S}	9.04 ± 0.06	7.10 ± 0.07	
$M_{L'}$	8.33 ± 0.12	6.783 ± 0.015	
M_{M_S}	9.3 ± 0.2	7.06 ± 0.05	

Table 4. Mass Estimates for HD 1160 BC

Parameter	Measurement	Mass (M_{Jup})
HD 1160 B		
M_J (mag)	10.75 ± 0.10	33^{+12}_{-9} ^a
M_H (mag)	9.57 ± 0.08	48^{+17}_{-13} ^a
M_{K_S} (mag)	9.04 ± 0.06	53^{+22}_{-15} ^a
$M_{L'}$ (mag)	8.3 ± 0.12	59^{+31}_{-10} ^a
M_{M_S} (mag)	9.3 ± 0.2	33^{+20}_{-12} ^a
BC_J	2.06 ± 0.14 ^b	37^{+12}_{-12} ^a
HD 1160 C		
Sp. Type	$M3.5 \pm 0.5$	
BC_K	2.72 ± 0.06 ^c	
Dwarf Temperature Scale		
T_{eff}	3270 ± 90 ^d	190^{+65}_{-40} ^e
Intermediate Temperature Scale		
T_{eff}	3340 ± 70 ^d	230^{+30}_{-45} ^e

^aChabrier et al. (2000)

^bLiu et al. (2010a)

^cGolimowski et al. (2004)

^dLuhman (1999)

^eBaraffe et al. (1998)